Treatment of simulated textile sludge using the Fenton/Cl$^-$ system: the roles of chlorine radicals and superoxide anions on PAHs removal

Xiaojun Lai, Xun-an Ning, Yaping Zhang, Yang Li, Riwen Li, Jiayi Chen, Shiyin Wu

PII: S0013-9351(21)00291-7

DOI: https://doi.org/10.1016/j.envres.2021.110997

Reference: YENRS 110997

To appear in: *Environmental Research*

Received Date: 16 December 2020

Revised Date: 20 February 2021

Accepted Date: 5 March 2021

Please cite this article as: Lai, X., Ning, X.-a., Zhang, Y., Li, Y., Li, R., Chen, J., Wu, S., Treatment of simulated textile sludge using the Fenton/Cl$^-$ system: the roles of chlorine radicals and superoxide anions on PAHs removal, *Environmental Research*, https://doi.org/10.1016/j.envres.2021.110997.

CRediT author statement

Xiaojun Lai: Conceptualization, Data curation, Formal analysis, Investigation, Methodology, Software, Writing - original draft preparation, Writing - review & editing. **Xun-an Ning:** Funding acquisition, Project administration, Supervision, Writing - review & editing. **Yaping Zhang:** Writing - review & editing. **Yang Li:** Writing - review & editing. **Riwen Li:** Investigation. **Jiayi Chen:** Investigation. **Shiyin Wu:** Investigation.

Treatment of simulated textile sludge using the Fenton/Cl^- system: the roles of chlorine radicals and superoxide anions on PAHs removal

Xiaojun Lai, Xun-an Ning*, Yaping Zhang, Yang Li, Riwen Li, Jiayi Chen, Shiyin Wu

Guangdong Key Laboratory of Environmental Catalysis and Health Risk Control, Institute of Environmental Health and Pollution Control, School of Environmental Science and Engineering, Guangdong University of Technology, Guangzhou 510006, China

*Corresponding author: **Prof. Xun-an Ning.**

Tel.: +86-20-3932 2546; Fax: 86-20-3932 2548; Email: ningxunan666@126.com; 1009560924@qq.com.

Abstract

The main content of this work is to investigate the removal of polycyclic aromatic hydrocarbons (PAHs: phenanthrene, anthracene, and fluoranthene) from simulated sludge solid phase employing an Fenton/Cl^- system under various Cl^- contents and pH values. The steady-state concentrations of the hydroxyl, chlorine, and dichloride anion radicals ($[\cdot OH]_{ss}$, $[\cdot Cl]_{ss}$, and $[Cl_2^{\cdot-}]_{ss}$) in heterogeneous system were first measured using *tert*-butanol, nitrobenzene, and benzoic acid. The outcomes exhibited that increasing the Cl^- content from 50 to 2000 mg/L (pH=3.0) or raising the pH from 3.0 to 5.0 (1000 mg/L Cl^-) caused $[\cdot OH]_{ss}$ to continuously decrease and $[Cl_2^{\cdot-}]_{ss}$ and the concentration of superoxide anions ($HO_2^{\cdot}/O_2^{\cdot-}$) to continuously increase. When the pH was 3.0 and the Cl^- concentration was 1000 mg/L, $[\cdot Cl]_{ss}$ had a maximum value of 9.27×10^{-14} M. Combining the results of PAH removal, radical quenching, and product analysis, it was found that $\cdot Cl$ in the Fenton/Cl^- system promoted the oxidative degradation of phenanthrene without forming chlorination byproducts. Furthermore, $HO_2^{\cdot}/O_2^{\cdot-}$ was helpful in removing anthracene and fluoranthene. Under the environment of high Cl^- content (≥1000 mg/L), PAHs could be removed more effectively by using $HO_2^{\cdot}/O_2^{\cdot-}$. This investigation underpins further study on the regulation of reactive species and the efficient degradation of target organic matter in Fenton/Cl^- system, and provides a basis for studying the formation of chlorinated or toxic byproducts in the process of treating textile dyeing sludge by Fenton.

Keywords: Textile dyeing sludge; Polycyclic aromatic hydrocarbons (PAHs); Fe^{2+}/H_2O_2

(Fenton); Chlorine radicals; Superoxide anions

1. Introduction

Textile dyeing sludge (TDS) is the most important byproduct of textile wastewater treatment stations and is the key source of secondary environmental pollution (Raheem et al., 2018). There are many pollutants in TDS, like polycyclic aromatic hydrocarbons (PAHs), dioxins, anilines, mono-benzene compound, and heavy metals (Table 1) (Krizanec and Le Marechal, 2006; Liang et al., 2017; Liang et al., 2013; Ning et al., 2015; Ning et al., 2014; Weng et al., 2012; Zhou et al., 2019; Zou et al., 2019). Among them, PAHs are priority pollutants primarily originating from dye impurities and dye conversion intermediates, which have health hazards such as toxic, carcinogenic and mutative (Lin et al., 2016). Our previous research exhibited that the majority of PAHs in TDS solid phase were three to four rings PAHs, such as anthracene (Ant), phenanthrene (Phe), and fluoranthene (Flu), and their contents were 9.54-2773.13 ng/g in dry sludge (DS), 9.91-2882.76 ng/g DS, and 16.96-4560.42 ng/g DS, respectively (Ning et al., 2014). The total content of PAHs in TDS exceeded the requirement of agricultural reuse of sludge (Table 1). Thus, efficient, environmentally friendly and sustainable treatment of TDS, especially PAHs in TDS, holds the key to sustainable development (Guan et al., 2018; Zhang et al., 2019b).

Table 1

PAHs have low biodegradability and are resistant to conventional treatments (Sanchez-Brunete et al., 2007), so advanced oxidation processes (AOPs) have been employed for degrading PAHs (Bendouz et al., 2017; Gu et al., 2018; Jia et al., 2018). The Fe^{2+}/H_2O_2 (Fenton) system is considered a typical AOP that can effectively destroy organic compounds (Zhu et al., 2019). Previous studies revealed that ferryl ions (Fe(□)), a reactive species, might exist in this system (Bataineh et al., 2012); however, Wang et al. (2020) employed a new method to explore and confirm that there were no Fe(□) present ($pH \leq 5.0$). Thus, the reactive species in the Fenton system are hydroxyl radicals (·OH: 2.8 V) and superoxide anions ($HO_2^{\cdot}/O_2^{\cdot -}$: 1.5 V) (He et al., 2016). The ·OH are the dominant reactive species that react with PAHs (free radical addition reaction), which are then converted into quinones and subsequently degraded (Lee et al., 2001). Flotron et al. (2005) used Fenton to degrade Flu, benzo[b]fluoranthene, and benzo[a]pyrene in the sludge solid phase, and showed that the maximum removal efficiency of benzo[a]pyrene was 67.00% under optimal conditions. Lin et al. (2016) used Fenton to degrade 16 kinds of PAHs detected in TDS solid phase, where the total PAH removal efficiency reached 83.50% when the amounts of H_2O_2 and Fe^{2+} were each 140 mM and the pH was 3.0.

Due to Cl^- in the textile wastewater and the use of chlorine-containing flocculants in wastewater treatment, Cl^- in the TDS (Cl^- concentration in liquid phase=54.13-1081.96 mg/L) cannot be ignored (Lai et al., 2020). Furthermore, Cl^- can react with H_2O_2 and ·OH in the Fenton system to form reactive chlorine species (RCS such as ·Cl, $Cl_2^{\cdot -}$, ·ClO, Cl_2, and HClO) (Eq. 1-12) (Fang et al., 2014; Meghlaoui et al., 2019; Nikravesh et al., 2020; Wu et al., 2019). However, our previous research (Lai et al., 2020) showed that free chlorine (Cl_2 and HClO) and ·ClO could not be detected in the Fenton/Cl^- system when the content of Cl^- was below 2000 mg/L. This may be because a large amount of H_2O_2 in the Fenton system reduced free chlorine (Eq. 13-14) (Crump et al., 1998). Therefore, the reactive species in the Fenton/Cl^- system ($Cl^- \leq 2000$ mg/L) include ·OH, ·Cl (2.47 V), $Cl_2^{\cdot -}$ (2.0 V) (Beitz et al., 1998) and $HO_2^{\cdot}/O_2^{\cdot -}$. Among them, ·Cl, $Cl_2^{\cdot -}$ and $HO_2^{\cdot}/O_2^{\cdot -}$ are selective radicals (Fang et al., 2014; He et al., 2016). It has been shown that free-radical RCS (·Cl, $Cl_2^{\cdot -}$, and ·ClO) play an important role in degrading trace pollutants, like trimethoprim, caffeine, and carbamazepine (Guo et al., 2017; Hua et al., 2019; Wu et al., 2016). Nevertheless, free-radical RCS may also cause chlorination byproducts to form (Huang et al., 2018; Lei et al., 2021; Yuan et al., 2011). Considering the entire course of disposal of TDS, if the concentration of chloride in the solid phase of sludge treated by the Fenton/Cl^- system increases, it will increase the risk of dioxin formation in subsequent incineration of TDS (Nganai et al., 2009; Wang et al., 2017); if products with greater toxicity than PAHs are formed in the sludge treated by the Fenton/Cl^- system, it will increase the environmental risk of TDS subsequent reuse and landfill (Liang et al., 2019). Then Fenton system could become a non-clean sludge treatment technology. At present, few studies have considered the oxidation or chlorination roles of free-radical RCS in the removal of organic matter using an Fenton/Cl^- system; therefore, this requires further study to determine whether Fenton is a clean treatment technology under the interference of Cl^-.

$$H_2O_2 + 2HCl \rightarrow Cl_2 + 2H_2O \qquad (1)$$

$$H_2O_2 + HCl \rightarrow HClO + H_2O \qquad (2)$$

$$\cdot \mathrm{OH} + Cl^- \leftrightarrow ClOH^{\cdot -}$$

$$K_+ = 4.3 \times 10^9 \ /Ms, \qquad K_- = 6.1 \times 10^9 \ /Ms \tag{3}$$

$$ClOH^{\cdot -} \leftrightarrow \cdot Cl + OH^-$$

$$K_+ = 2.0 \times 10^{10} \ /Ms, \qquad K_- = 1.8 \times 10^{10} \ /Ms \tag{4}$$

$$\cdot Cl + Cl^- \leftrightarrow Cl_2^{\cdot -}$$

$$K_+ = 6.5 \times 10^9 \ /Ms, \qquad K_- = 1.1 \times 10^5 \ /Ms \tag{5}$$

$$\cdot Cl + HClO \rightarrow \cdot ClO + HCl$$

$$K_+ = 3.0 \times 10^9 \ /Ms \tag{6}$$

$$Cl_2^{\cdot -} + OH^- \leftrightarrow ClOH^{\cdot -} + Cl^-$$

$$K_+ = 7.3 \times 10^6 - 4.5 \times 10^7 \ /Ms, \qquad K_- = 1.0 \times 10^5 \ /Ms \tag{7}$$

$$\cdot OH + HClO \leftrightarrow \cdot ClO + H_2O$$

$$K_+ = 2.0 \times 10^9 \ /Ms \tag{8}$$

$$Cl_2^{\cdot -} + Cl_2^{\cdot -} \rightarrow Cl_2 + 2Cl^-$$

$$K_+ = 6.3 \times 10^8 \ /Ms \tag{9}$$

$$\cdot Cl + \cdot Cl \rightarrow Cl_2$$

$$K_+ = 8.8 \times 10^7 \ /Ms \tag{10}$$

$$\cdot Cl + Cl_2^{\cdot -} \rightarrow Cl_2 + Cl^-$$

$$K_+ = 2.1 \times 10^9 \ /Ms \tag{11}$$

$$\cdot OH + Cl_2^{\cdot -} \rightarrow HClO + Cl^-$$

$$K_+ = 1.0 \times 10^9 \ /Ms \tag{12}$$

$$H_2O_2 + Cl_2 \rightarrow 2HCl + O_2 \tag{13}$$

$$H_2O_2 + HClO \rightarrow HCl + O_2 + H_2O \quad (14)$$

As was mentioned, the reactive species in the Fenton/Cl^- system ($Cl^- \leq 2000$ mg/L) include ·OH, ·Cl, $Cl_2^{\cdot -}$, and $HO_2^{\cdot}/O_2^{\cdot -}$. The formation and concentration of those reactive species are obviously influenced by pH and Cl^- concentration (Hua et al., 2019; Zhu et al., 2019). Cl^- concentration and pH affect the transformation speed among ·OH, ·Cl, and $Cl_2^{\cdot -}$ (Fang et al., 2014; Lai et al., 2020; Wu et al., 2019). Cl^- concentration and pH also affect the morphology of $HO_2^{\cdot}/O_2^{\cdot -}$ and the cycle of Fe^{3+} and Fe^{2+} ions, which consequently affects the formation and concentrations of ·OH and $HO_2^{\cdot}/O_2^{\cdot -}$ (Jung et al., 2009; Xu et al., 2017; Zhu et al., 2019). Furthermore, the mechanism by which organic matter is removed is affected by the type of reactive species and its concentration. Thus, it's essential to further investigate how pH and Cl^- concentration affects the reactive species concentration and the removal of PAHs with diversified structures.

The main research objectives of this work were as follows: 1) to assess the influence of Cl^- concentration and pH on the removal degree and removal kinetics of PAHs (Phe, Ant, and Flu) from the solid phase of simulated sludge using an Fenton/Cl^- system; 2) to clarify the dominant reactive species (·OH, ·Cl, $Cl_2^{\cdot -}$, or $HO_2^{\cdot}/O_2^{\cdot -}$) in the Fenton/$Cl^-$ system under various Cl^- contents and pH and to explore how these parameters affect the steady-state contents of ·OH, ·Cl, and $Cl_2^{\cdot -}$ ($[\cdot OH]_{ss}$, $[\cdot Cl]_{ss}$, and $[Cl_2^{\cdot -}]_{ss}$); 3) to analyze the relationship between reactive species and the removal efficiency of PAHs or the first-order rate constant of PAHs removal; and 4) to observe the structure and toxicity of intermediate products of Phe degradation in the Fenton/Cl^- system and to explore whether

Phe and its intermediate products are chlorinated.

2. Materials and methods

2.1. Reagents

Standard solutions of Phe, Ant, Flu, and phenanthrene-D10 (as an internal standard) as well as a mixed standard solution of fluorine-D10 and pyrene-D10 (as surrogate standards) with purities >99.5% came from O2Si Smart Solutions (Charleston, SC, USA). Nitrobenzene (NB; purity>99.8%), benzoic acid (BA) standard solid (purity>99.9%), *tert*-butyl alcohol (TBA; purity>99.5%), *p*-benzoquinone (BQ; purity>99.5%), 5,5-dimethyl-1-pyrroline-*N*-oxide (DMPO; purity>97%), dimethyl sulfoxide (DMSO; purity>99.5%), polymeric ferric sulfate (PFS), $FeSO_4 \cdot 7H_2O$, anhydrous sodium acetate, *N*,*O*-bis-(trimethylsilyl)-trifluoroacetamide (BSTFA), and pyridine came from Macklin Company. H_2O_2 and H_2SO_4 were purchased from Guangzhou Brand Reagent Company, and NaCl, CaO, $Na_2HPO_4 \cdot 12H_2O$, NaOH, SiO_2, sodium hyposulfite, and anhydrous sodium sulfate came from the Tianjin Damao Reagent Company. Other high-performance liquid chromatography (HPLC) grade organic reagents came from ANPEL Laboratory Technologies Company. All inorganic reagents were of analytical grade or guaranteed grade and need not be further purified.

2.2. Solid phase of simulated textile dyeing sludge

In our previous research, PFS solution was mixed with inorganic compounds such as CaO, $NaHPO_4$, SiO_2 and NaOH, then the mixture was centrifuged, and finally the solid phase of the mixture was freeze-dried (-60 □, 24 h) to prepare the solid phase of simulated sludge (Lai et al., 2019; Liang et al., 2019). In this investigation, on basis of the TDS elemental content (Lai et al., 2020) and the preparation method of simulated sludge solid phase, the simulated sludge solid phase without PAHs was obtained and exhibited a similar inorganic composition and physical structure (particle size, microstructure, etc.) to those of TDS (Lai et al., 2019; Liang et al., 2019). The relative content of elements in the solid phase of simulated sludge is shown in Table S1.

2.3. Experimental procedure

Under different conditions (pH, Cl^- concentration, reaction time and quencher), Fenton/Cl^- system was used to treat the PAHs in simulated sludge solid phase and the probes of reactive species (NB, BA, TBA, DMPO) in simulated sludge liquid phase. A more detailed description is shown in Text S1.

2.4. Analytical approaches

The NB and BA were analyzed by HPLC. Gas chromatography-mass spectrometry (GC-MS) was used to analyze TBA, PAHs and PAHs products. The concentration of $HO_2^{\cdot}/O_2^{\cdot-}$ was analyzed by electron paramagnetic resonance (EPR). The chronic and acute toxicity of Phe and its products were predicted by ECOSAR program. More detailed analytical methods are shown in Text S2.

2.5. Quality assurance and control

All experiments were performed in the dark. Each experiment was repeated three or more times, and each batch of degradation experiments had a control sample without degradation treatment. Routine analysis of PAH substitutes (fluorine-D10 and pyrene-D10), spiked blanks, and program blanks was carried out. The recoveries of Phe, Ant, and Flu were 116.05±2.87%, 80.21±2.92%, and 113.11±1.63%, respectively, whereas the recoveries of fluorine-D10 and pyrene-D10 in samples were 80.68±3.73% and 109.19±7.13%, respectively.

3. Results and discussion

3.1 Effects of Cl^- content and pH on PAH removal from simulated sludge

Fig. 1

In real situations, the factors affecting the removal of 16 PAHs from TDS by the Fenton system can be divided into three categories: reaction conditions, solid-phase properties of sludge and liquid-phase impurities of sludge. The reaction conditions include the ratio of Fe^{2+} to H_2O_2 (1:9 to 1.5:1), H_2O_2 dosage (20-180 mM), pH (2.0-6.8) and reaction time (5-60 min) (Lin et al., 2016). Solid properties of sludge include particle size, microstructure and organic composition (organic matter polarity, aromatic carbon content and fatty carbon content) (Ke et al., 2018; Liang et al., 2017). The impurities in sludge liquid phase include humus and inorganic ions (Cl^-, SO_4^{2-}, HCO_3^-, HPO_4^-, SiO_3^{2-}) (Lai et al., 2019; Ribeiro et al., 2019). TDS is a very complex system, but in this study, the TDS is simplified, which can clarify the mechanism of the influence of Cl^- concentration and pH in the Fenton/Cl$^-$ system on the removal of PAHs with different structures.

Our previous research (Lai et al., 2020) determined the best reaction conditions (H_2O_2/Fe^{2+}=1/1, H_2O_2=30 mM) for removing Phe, Ant, and Flu from simulated sludge solid phase using an Fenton system at initial pH=7.0. Because of the contact limitation between reactive species in liquid phase and PAHs in solid phase (Lin et al., 2016), the dosage of H_2O_2 in simulated sludge research was higher than that in simulated wastewater research (Bendouz et al., 2017). Then, under these reaction conditions (H_2O_2/Fe^{2+}=1/1, H_2O_2=30 mM, pH=3.0), the effect of Cl$^-$ concentration (50-2000 mg/L) on PAH removal from simulated sludge solid phase using the Fenton/Cl$^-$ system was explored (Fig. 1). As shown in Figs. 1(a)-(d), the PAH removal efficiencies increased with increasing reaction time. When the reaction time exceeded 30 min, the PAHs had no obvious change in removal efficiency. This was because the oxidation ability of the system was too weak to degrade PAHs after 30 min, which was similar to previous studies (Lin et al., 2016; Sun and Yan, 2008). Therefore, the influences of Cl$^-$ concentration on the PAH removal efficiency were examined with reaction times of 40 min. When the content of Cl$^-$ was low (50 mg/L), the order of the PAH removal efficiencies (over 40 min) was Ant (85.47±0.99%)>Flu (62.95±0.22%)≈Phe (63.16±1.86%). Increasing the Cl$^-$ concentration initially increased the removal efficiencies of Phe and Flu, after which they decreased. When the content of Cl$^-$ was 1000 mg/L, the removal efficiencies of Phe and Flu reached their maximum values of 88.61±0.07% and 82.36±1.61%, respectively. When the content of Cl$^-$ was ≤500 mg/L, increasing Cl$^-$ content didn't affect the removal efficiency of Ant.

However, when the content of Cl^- was ≥1000 mg/L, increasing Cl^- content obviously decreased the removal efficiency of Ant. When the concentration of Cl^- was 2000 mg/L, the removal efficiency of Ant was the lowest (53.91±0.44%). In addition, when the content of Cl^- was ≤1000 mg/L, the total PAH removal efficiency exhibited negligible changes. This was because the Cl^- concentration had different effects on PAHs with different structures, and the final phenomenon was that the total PAHs removal had no obvious change (Cl^- ≤1000 mg/L).

Fig. 2

Anhydrous sodium acetate was employed as a pH buffer in the Fenton/Cl^- system (Wang et al., 2019). How pH affects the removal of PAHs from simulated sludge solid phase using this system is exhibited in Fig. 2. As pH increased, the removal efficiencies of Phe and Flu didn't obviously alter, but the removal efficiency of Ant clearly increased. When the pH was raised from 3.0 to 5.0, the removal efficiency of Ant increased from 63.61±1.40% to 85.88±0.08% after 40 min. The removal efficiency of Phe and Flu was not obviously affected by pH, so the total PAH removal efficiency was not significantly altered with increasing pH value. Generally speaking, in the acidic and proper Cl^- content (≤1000 mg/L) environment, the change of pH and Cl^- content had little influence on the removal degree of total PAHs. However, in the environment with high Cl^- content, it may be more beneficial to remove total PAHs by properly adjusting the environmental pH to weak acidity.

The data in Fig. 1 and Fig. 2 were further analyzed, and the first-order rate constants of PAH removal are shown in Table 2. Since the oxidation ability of the Fenton/Cl^- system was too weak to degrade PAHs after 30 min, the kinetic analysis focused on the reaction before 30 min. When pH=3.0, increasing Cl^- concentration caused the first-order rate constants of Phe and Flu removal to first decrease, then increase, and finally decrease again. Contrastingly, the first-order rate constant of Ant removal continuously decreased. When the pH was 3.0 and the concentration of Cl^- was 1000 mg/L, the first-order rate constants of Phe and Flu removal had the largest values, which were 7.75×10^{-4} /s and 6.17×10^{-4} /s, separately. When the pH was 3.0, the change in the first-order rate constant of total PAH removal was consistent with those of Phe and Flu as Cl^- concentration increased. When the content of Cl^- was 1000 mg/L and the pH of the system was increased to 5.0, the first-order rate constants of Phe and Flu removal decreased to 0.17 times and 0.14 times, respectively. Additionally, the first-order rate constant of Ant removal increased to 1.02 times, and the change in the first-order rate constant of total PAH removal was consistent with those of Phe and Flu.

Table 2

To sum up, under the condition that the concentration of Cl^- can be controlled, according to the efficiency and first-order rate constants of Phe, Ant and Flu removal, it is necessary to keep the system at a low pH value (pH=3.0) and an appropriate Cl^- content (e.g. 1000 mg/L) in order to remove all kinds of PAHs quickly and simultaneously.

3.2 Contribution of reactive species to PAH removal from simulated sludge solid phase

Before the formal experiment, the concentration of free chlorine in the Fenton/Cl^-

system was determined. The results show that there was no free chlorine in the Fenton/Cl^- system under different conditions (pH=3.0-5.0, Cl^- =50-2000 mg/L) (Eq. 13-14), which was similar to previous studies (Lai et al., 2020).

Table 3

Fig. 3

However, the formation of $\cdot Cl$ and $Cl_2^{\cdot -}$ in the Fenton/Cl^- system results from the reaction of $\cdot OH$ with Cl^- (Eq. 3-5), and TBA can quench $\cdot OH$ and hinder these formations. In this study, TBA and BQ were used to quench $\cdot OH$, $\cdot Cl$, $Cl_2^{\cdot -}$, and $HO_2^{\cdot}/O_2^{\cdot -}$ species in the reaction system. The second-order rate constants of the reactions between TBA, BQ, and these reactive species are exhibited in Table 3 (Fang et al., 2014; Hasegawa and Neta, 1978; He et al., 2016; Hua et al., 2019; Li et al., 2020; Ma et al., 2019; NDRL/NIST, 2017; Varanasi et al., 2018; Watts and Teel, 2019). The reactive species contribute to PAH removal, as exhibited in Fig. 3. Additionally, PAH volatilization may be partially responsible for low PAH removal (Fig. 3: Other). Fig. 3(a) exhibited that as Cl^- content increases, the contribution of $HO_2^{\cdot}/O_2^{\cdot -}$ to Phe removal increased. When the content of Cl^- was 2000 mg/L, $HO_2^{\cdot}/O_2^{\cdot -}$ contributed to 39.37% of total Phe removal. As Cl^- concentration increased, the contributions of $\cdot OH$, $\cdot Cl$, and $Cl_2^{\cdot -}$ to Phe removal first increased and then decreased. These contributions were largest when the concentration of Cl^- was 1000 mg/L, where they accounted for 90.81% of total Phe removal. Thus, as Cl^- concentration increases, the removal efficiency of Phe over 40 min first increased and then decreased because the combined contributions of $\cdot OH$, $\cdot Cl$, and $Cl_2^{\cdot -}$ also initially increased and then decreased. Varying the Cl^- concentration caused changes in the actions of the ·OH, ·Cl, and $Cl_2^{\cdot-}$ species, which consequently altered the Phe removal efficiency.

As shown in Fig. 3(b), the contribution of $HO_2^{\cdot}/O_2^{\cdot-}$ to Ant removal increased slightly with increasing Cl^- concentration. When Cl^- content was ≥1000 mg/L, the contributions of ·OH, ·Cl, and $Cl_2^{\cdot-}$ to Ant removal decreased significantly. These contributions to Ant removal were smallest when Cl^- content was 2000 mg/L, accounting for 17.57% of the total Ant removal. Thus, when Cl^- content was ≥1000 mg/L, the removal efficiency of Ant (over 40 min) decreased because the combined actions of ·OH, ·Cl, and $Cl_2^{\cdot-}$ decreased. As Cl^- concentration varied, the change in the Ant removal efficiency was primarily affected by changes in the actions of the ·OH, ·Cl, and $Cl_2^{\cdot-}$ species.

Furthermore, Fig. 3(c) shows that increasing Cl^- concentration significantly increased the contribution of $HO_2^{\cdot}/O_2^{\cdot-}$ to Flu removal. When Cl^- content was 2000 mg/L, $HO_2^{\cdot}/O_2^{\cdot-}$ contributed to 86.72% of the total Flu removal. Thus, because the action of $HO_2^{\cdot}/O_2^{\cdot-}$ increased as Cl^- content rises, the removal efficiency of Flu (over 40 min) first increased. However, it subsequently decreased due to the combined actions of ·OH, ·Cl, and $Cl_2^{\cdot-}$ decreasing at high Cl^- concentrations (2000 mg/L). As Cl^- concentration varied, the change in the Flu removal efficiency was related to changes in the contribution of all reactive species.

Fig. 4

As shown in Fig. 4, the $HO_2^{\cdot}/O_2^{\cdot-}$ species in the Fenton/Cl^- system was analyzed by

EPR. It was found that increasing Cl^- concentration caused the DMPO-OOH adduct signal to increase (Chen et al., 2017), and it increased the concentration of $HO_2^{\cdot}/O_2^{\cdot -}$ in the Fenton/Cl^- system. Cl^- complexed with Fe^{3+} in the Fenton/Cl^- system and its complexation strength was greater than that of OH^- and Fe^{3+} complexation (Lu et al., 2005; Wang and Xu, 2003), which could reduce the speed by which $HO_2^{\cdot}/O_2^{\cdot -}$ and Fe^{3+} react. In addition, the reaction between Fe^{3+} and H_2O_2 was very slow (0.001-0.01 /Ms, 25 □, aqueous phase, no catalyst), which was the speed-limiting step of the Fenton system (Zhu et al., 2019); therefore, the formation of $HO_2^{\cdot}/O_2^{\cdot -}$ was not significantly affected by Fe^{3+} complexation with Cl^-. Overall, considering the formation and reaction of $HO_2^{\cdot}/O_2^{\cdot -}$, increasing Cl^- concentration increased the content of $HO_2^{\cdot}/O_2^{\cdot -}$ in the Fenton/Cl^- system and the contribution of $HO_2^{\cdot}/O_2^{\cdot -}$ to PAH removal. Changes in the concentrations of $\cdot OH$, $\cdot Cl$, and $Cl_2^{\cdot -}$ will be discussed in the following sections.

When the pH was ≥4.0 (Fig. 3(a)-(c)), the PAH removal was mainly attributed to the oxidation of $HO_2^{\cdot}/O_2^{\cdot -}$. This was because the concentration of $HO_2^{\cdot}/O_2^{\cdot -}$ increased with increasing pH (Fig. 4). High Cl^- concentration (1000 mg/L) and high pH (≥4.0) were unfavorable for $HO_2^{\cdot}/O_2^{\cdot -}$ to reduce Fe^{3+}. With the decrease in iron-ion circulation, the $\cdot OH$ concentration decreased and the $HO_2^{\cdot}/O_2^{\cdot -}$ concentration increased. When the pH raised from 3.0 to 5.0, the removal efficiency of Phe and Flu (over 40 min) exhibited negligible changes because of the great increase of $HO_2^{\cdot}/O_2^{\cdot -}$ contribution. Under similar conditions, the removal efficiency of Ant increased because the oxidation of Ant by $HO_2^{\cdot}/O_2^{\cdot -}$ at a pH of 4.0-5.0 was stronger than the Ant oxidation provided by all reactive species at a pH of 3.0. Therefore, due to the action of $HO_2^{\cdot}/O_2^{\cdot -}$, increasing pH does not inhibit Phe and Flu removal, but it facilitates Ant removal. In addition, in the environment with high Cl^- content (≥1000 mg/L), it is more effective to degrade PAHs in TDS with $HO_2^{\cdot}/O_2^{\cdot -}$.

Comparing Figs. 3 (a), (b), and (c), it was found that when the pH was 3.0 and the Cl^- concentration was 50 mg/L, the contribution of $HO_2^{\cdot}/O_2^{\cdot -}$ to Ant removal was the largest. This indicated that the reactivity of $HO_2^{\cdot}/O_2^{\cdot -}$ was greater with Ant than with Phe or Flu. With an increase in Cl^- from 50 to 1000 mg/L, the concentration of $HO_2^{\cdot}/O_2^{\cdot -}$ also increased, but the contribution of $HO_2^{\cdot}/O_2^{\cdot -}$ to Ant removal exhibited little change. This could be due to the high reactivity of ·OH and Ant in the degradation system (Lai et al., 2020), which caused the small decrease in $[\cdot OH]_{ss}$ and the small increase in $HO_2^{\cdot}/O_2^{\cdot -}$ concentration to have little influence on Ant removal. Moreover, with increasing Cl^- concentration, the contribution of $HO_2^{\cdot}/O_2^{\cdot -}$ to Flu removal greatly increased. This shows that the reactivity of ·OH is lower with Flu than with Ant, but $HO_2^{\cdot}/O_2^{\cdot -}$ also demonstrated strong reactivity with Flu. Therefore, a small increase in the concentration of $HO_2^{\cdot}/O_2^{\cdot -}$ had significant influence on Flu removal. The reactivity of $HO_2^{\cdot}/O_2^{\cdot -}$ with the PAHs was in the order of Ant>Flu>Phe.

3.3 The steady-state concentrations of the ·OH, ·Cl and $Cl_2^{\cdot -}$ species

3.3.1 Determining steady-state concentrations (0.5-30 min) of ·OH, ·Cl, and $Cl_2^{\cdot -}$

The ·OH species in the Fenton/Cl^- system can react with Cl^- for forming free-radical

RCS (·Cl and $Cl_2^{\cdot -}$) (Fang et al., 2014; Wu et al., 2019). Contrastingly, $HO_2^{\cdot}/O_2^{\cdot -}$ cannot accomplish this because of its weak oxidation ability (He et al., 2016). Therefore, as Cl^- concentration and pH increase, $[\cdot OH]_{ss}$, $[\cdot Cl]_{ss}$, and $[Cl_2^{\cdot -}]_{ss}$ may change, as well as the contributions of ·OH, ·Cl, and $Cl_2^{\cdot -}$ to PAH removal. In this study, NB (19.14 μg/mL), TBA (31.00 μg/mL), and BA (40.00 μg/mL) were used to measure $[\cdot OH]_{ss}$, $[\cdot Cl]_{ss}$, and $[Cl_2^{\cdot -}]_{ss}$. These values were obtained according to the formulas in Eq. 15-17 (Hua et al., 2019). The second-order rate constants of the reactions between NB, BA, TBA, and reactive species are shown (Table 3). Previous studies have shown that NB, BA, and TBA do not react with $HO_2^{\cdot}/O_2^{\cdot -}$ (Table 3) (Ma et al., 2019; Watts and Teel, 2019). Thus, $HO_2^{\cdot}/O_2^{\cdot -}$ did not interfere with the determination of $[\cdot OH]_{ss}$, $[\cdot Cl]_{ss}$, and $[Cl_2^{\cdot -}]_{ss}$ in this study. The degradation system in this study was heterogeneous (containing simulated sludge solid phase), so the adsorption of simulated sludge solid phase was also considered. In addition, previous studies have shown that the Fenton reaction process consists of two stages: Fe^{2+}/H_2O_2 and Fe^{3+}/H_2O_2 (Lu et al., 2005; Zhu et al., 2019). In the first stage, Fe^{2+} quickly reacts with H_2O_2, a large amount of ·OH is produced, and organic matter is rapidly degraded. Since Fe^{2+} reacts very rapidly with H_2O_2, this study mainly explores the kinetics of PAH removal and the steady-state contents of free radicals in the second stage (0.5-30 min) of the Fenton/Cl^- system.

$$K_{NB}^{1} = K_{adsorption-NB}^{1} + K_{\cdot OH-NB} \times [\cdot OH]_{ss} \tag{15}$$

$$K_{TBA}^{1} = K_{adsorption-TBA}^{1} + K_{\cdot OH-TBA} \times [\cdot OH]_{ss} + K_{\cdot Cl-TBA} \times [\cdot Cl]_{ss} \tag{16}$$

$$K_{BA}^{1} = K_{adsorption-BA}^{1} + K_{\cdot OH-BA} \times [\cdot OH]_{ss} + K_{\cdot Cl-BA} \times [\cdot Cl]_{ss} + K_{Cl_2^{\cdot -}-BA} \times [Cl_2^{\cdot -}]_{ss} \tag{17}$$

where K^1 represents the first-order rate constant (/s) and K indicates the second-order rate constant (/Ms).

Fig. 5

As shown in Fig. 5, NB (hydrophobic organic matter), BA (weak acid), and TBA (hydrophilic organic matter) in the system liquid phase were adsorbed by the simulated sludge solid phase under different pH conditions. As pH increased, the first-order adsorption rate constant of NB showed little change, while that of TBA increased. When the pH was 4.0, the first-order adsorption rate constant of BA had a minimum value of 2.49×10^{-5} /s. Therefore, pH exhibited a weak influence on NB adsorbed onto the solid phase of simulated sludge by the hydrophobic effect. As the pH decreased, the solid structure of simulated sludge was destroyed and the amount of TBA adsorbed by the solid phase of simulated sludge (via hydrogen bonding) dropped. With the pH increasing, BA changed from its protonated state to its ionic state (pKa=4.20) (Karunanayake et al., 2017), causing a drop in the amount of BA adsorbed by the simulated sludge solid phase. When the pH was 5.0, the adsorption capacity of BA by the simulated sludge solid phase increased slightly because of the enhanced electrostatic adsorption of the simulated sludge solid phase. Fig. S1 exhibited that NB, BA, and TBA in the simulated sludge liquid phase were removed by the Fenton/Cl^- system with different Cl^- concentrations and pH values. According to Fig. 5, Fig. S1, Table 3, and Eq. 15-17, $[\cdot OH]_{ss}$, $[\cdot Cl]_{ss}$, and $[Cl_2^{\cdot -}]_{ss}$ in the Fenton/Cl^- system were calculated (Fig. 6).

3.3.2 The relationship between the steady-state concentration of free radicals and PAH removal

Fig. 6

Figure 6(a) exhibited that when Cl^- content rose from 50 to 2000 mg/L, $[\cdot OH]_{ss}$ decreased from 8.14×10^{-14} to 1.42×10^{-14} M while $[Cl_2^{\cdot-}]_{ss}$ increased from 5.14×10^{-12} to 1.01×10^{-9} M. The value of $[\cdot Cl]_{ss}$ was the highest (9.27×10^{-14} M) when the concentration of Cl^- was 1000 mg/L. Wu et al. (2019) studied the steady-state content of free radicals in a $UV/S_2O_8^{2-}/Cl^-$ system ($S_2O_8^{2-}$ =0.5 mM; pH=7.0) by simulation calculations and found that $[\cdot Cl]_{ss}$ peaked at a value of $1.5\text{-}2.0\times10^{-14}$ M when the concentration of Cl^- was 3.55-35.45 mg/L. Furthermore, the results of this study have trends similar to those seen in the work of Wu et al. (2019). In this study, the reaction between $\cdot OH$ and Cl^- was accelerated (Eq. 3) and the formation of free-radical RCS ($\cdot Cl$ and $Cl_2^{\cdot-}$) increased (Eq. 4-5) when the Cl^- concentration was increased, which caused $[\cdot OH]_{ss}$ to decrease. In addition, when Cl^- content was 2000 mg/L, $\cdot Cl$ reacted with a large amount of Cl^- and was converted into $Cl_2^{\cdot-}$ (Eq. 5), which resulted in $[\cdot Cl]_{ss}$ decreasing. At this time, $[Cl_2^{\cdot-}]_{ss}$ (1.01×10^{-9} M) was five orders of magnitude larger than both $[\cdot OH]_{ss}$ (1.42×10^{-14} M) and $[\cdot Cl]_{ss}$ (3.06×10^{-14} M). However, under similar conditions, the co-contribution of $\cdot OH$, $\cdot Cl$, and $Cl_2^{\cdot-}$ to Phe, Ant, and Flu removal was at its lowest (Fig 3). Therefore, the reactivity of $Cl_2^{\cdot-}$ with PAHs is inferior to that of $\cdot OH$ with PAHs. Additionally, the removal of PAHs by $Cl_2^{\cdot-}$ can be neglected. When Cl^- content was 1000 mg/L, the value of $[\cdot Cl]_{ss}$ (9.27×10^{-14} M) was the highest, and the co-contribution of $\cdot OH$, $\cdot Cl$, and $Cl_2^{\cdot-}$ to Phe removal was the greatest

(Fig. 3(a)). This suggests that the reactivity of $\cdot$Cl with Phe is greater than that of $\cdot$OH with Phe. However, when Cl^- content was 1000 mg/L, the co-contribution of $\cdot$OH, $\cdot$Cl, and $Cl_2^{\cdot -}$ to Ant removal was greatly reduced, indicating that the reactivity of $\cdot$Cl with Ant is inferior to that of $\cdot$OH with Ant. When Cl^- content was 50-1000 mg/L, the co-contribution of $\cdot$OH, $\cdot$Cl, and $Cl_2^{\cdot -}$ to Flu removal exhibited little change; thus, the reactivity of $\cdot$Cl with Flu may be equal to that of $\cdot$OH with Flu. The reactivity of $\cdot$Cl with the PAHs is in the order of Phe>Flu>Ant. In addition, as the removal of PAHs by $Cl_2^{\cdot -}$ can be neglected, $Cl_2^{\cdot -}$ will not be considered in the subsequent discussion.

As Cl^- concentration increased, the first-order rate constant of Phe removal first decreased, then increased, and then decreased again. This might be because when Cl^- content was 50 mg/L, the $[\cdot OH]_{ss}$ value was the highest (8.14×10^{-14} M), so the rate of Phe removal over 5-30 min was fast. However, when Cl^- content was 100-500 mg/L, the system was dominated by $\cdot$OH and the value of $[\cdot OH]_{ss}$ decreased. This caused the removal of Phe (over 5-30 min) to slow down. When Cl^- content was 1000 mg/L the degradation system was dominated by $\cdot$Cl ($[\cdot Cl]_{ss}=9.27\times10^{-14}$ M), which provided the fastest rate of Phe removal. When Cl^- content was 2000 mg/L, $[\cdot OH]_{ss}$ and $[\cdot Cl]_{ss}$ decreased and the rate of Phe removal subsequently slowed down again.

Increasing Cl^- concentration caused the first-order rate constant of Ant removal to decrease, which was the result of low reactivity of $\cdot$Cl with Ant, $[\cdot OH]_{ss}$ decreasing and the contribution of $HO_2^{\cdot}/O_2^{\cdot -}$ negligibly changing. Increasing Cl^- concentration also caused the first-order rate constant of Flu removal to initially decrease, then increase, and then decrease again. However, unlike Phe, the removal of Flu was obviously affected by $HO_2^{\cdot}/O_2^{\cdot -}$ (Fig. 3). The value of $[\cdot OH]_{ss}$ was the highest when Cl^- content was 50 mg/L, which made for the rapid removal of Flu over 5-30 min. However, when Cl^- content was 100-500 mg/L, the system was dominated by $HO_2^{\cdot}/O_2^{\cdot -}$ and $\cdot OH$, and the reaction between $HO_2^{\cdot}/O_2^{\cdot -}$ and Flu was slow. This reduced the speed of Flu removal. When Cl^- content was 1000 mg/L, the system was dominated by $HO_2^{\cdot}/O_2^{\cdot -}$ and $\cdot Cl$. Furthermore, the total steady-state contents of $\cdot Cl$ and $\cdot OH$ when Cl^- content was 1000 mg/L were 2.09 times greater than those when Cl^- content was 500 mg/L, which caused Flu removal to suddenly accelerate. When Cl^- content was 2000 mg/L, the system was dominated by $HO_2^{\cdot}/O_2^{\cdot -}$ and the rate of Flu removal again slowed.

When the pH increased from 3.0 to 5.0, $[\cdot OH]_{ss}$ decreased from 2.62×10^{-14} to 2.82×10^{-16} M, $[\cdot Cl]_{ss}$ decreased from 9.27×10^{-14} to 2.66×10^{-14} M, and $[Cl_2^{\cdot -}]_{ss}$ increased from 5.09×10^{-10} to 1.31×10^{-9} M (Fig. 6(b)). As pH increased, the peak value of $[\cdot Cl]_{ss}$ shifted in the direction of low Cl^- concentration; therefore, the first-order rate constants of Phe and Flu removal decreased because the values of $[\cdot OH]_{ss}$ and $[\cdot Cl]_{ss}$ decreased. Although the concentration of $HO_2^{\cdot}/O_2^{\cdot -}$ increased with an increase in pH (Fig. 4), the reaction of $HO_2^{\cdot}/O_2^{\cdot -}$ with Phe and Flu was slow. With the pH increasing from 3.0 to 4.0, the first-order rate constant of Ant removal also increased due to the concentration of $HO_2^{\cdot}/O_2^{\cdot -}$ increasing, which again demonstrates the strong reactivity of Ant with $HO_2^{\cdot}/O_2^{\cdot -}$.

Generally, different Cl^- concentrations and pH values in the Fenton/Cl^- system have affected PAH removal in different ways, which is primarily due to the different reactivity of PAHs with ·Cl, $Cl_2^{\cdot -}$, and $HO_2^{\cdot}/O_2^{\cdot -}$. Therefore, the outcomes of this investigation exhibit that the main reactive species in the Fenton/Cl^- system can be controlled by regulating the Cl^- concentration and pH value. Furthermore, the selective and efficient degradation of some trace organic matter can be realized. When the target pollutants in the system have high reactivity with ·OH (e.g., Ant), it is necessary to maintain the pH and Cl^- concentration of the Fenton/Cl^- system at low values. When the target pollutants in the system have high reactivity with ·Cl (e.g., Phe), the pH and Cl^- concentration of the Fenton/Cl^- system must be kept within an appropriate range. Moreover, when the target pollutants in the system do not react with ·OH (e.g., carbon tetrachloride or chloroform) (Smith et al., 2006), have poor water solubility (Smith et al., 2015), or have high reactivity with $HO_2^{\cdot}/O_2^{\cdot -}$, it is necessary to increase the pH or Cl^- concentrations of the Fenton/Cl^- system. However, if the original Cl^- content in TDS is high and ·OH or ·Cl in the Fenton/Cl^- system is greatly converted into $Cl_2^{\cdot -}$, the micro-acid environment is more effective in removing organic matter by using $HO_2^{\cdot}/O_2^{\cdot -}$.

It is worth noting that a large amount of saline wastewater entering the environment will lead to soil salinization, plant growth retardation and biological poisoning (Hu et al., 2013). Therefore, adding Cl^- during sludge treatment may increase the desalination pressure of wastewater treatment plants. The practical application of the Fenton/Cl^- system needs further research and consideration. However, this study can prove that the original Cl^- in the system is not necessarily unfavorable to the removal of organic matter, and put forward the solution to remove organic matter under the condition of high Cl^-.

3.4 Structure and toxicity analysis of Phe products

According to the aforementioned experimental results, when Cl^- content was 1000 mg/L, the value of $[\cdot Cl]_{ss}$ in the Fenton/Cl^- system (H_2O_2/Fe^{2+}=1/1, H_2O_2=30 mM, pH=3.0) was the highest. Furthermore, the reactivity of ·Cl with Phe was greater than that of ·OH with Phe. Alegre (2000) and Martire (2001) et al. showed that chlorination byproducts might be formed by the reaction of ·Cl with organic compounds (free radical addition). Therefore, the degradation of Phe in the simulated sludge by the Fenton/Cl^- system (H_2O_2/Fe^{2+}=1/1, H_2O_2=30 mM, Cl^- =1000 mg/L, pH=3.0) was likely to form chlorinated byproducts. To identify the degradation products of Phe, the reaction conditions were all quadrupled (H_2O_2/Fe^{2+}=1/1, H_2O_2=120 mM, Cl^- =4000 mg/L, pH=3.0, 1-30 min) for degrading the simulated sludge containing high content of Phe. The degradation products of Phe in the Fenton/Cl^- system were identified by GC-MS and are available from Table S2, Fig. S2, and Fig. S3.

The Fenton/Cl^- system (H_2O_2/Fe^{2+}=1/1, H_2O_2=30 mM, Cl^- =4000 mg/L, pH=3.0) was used to treat high concentrations of Phe in the simulated sludge, and the removal efficiency of Phe from the simulated sludge solid phase was 87.24% (30 min). Within 1 min, Phe in the liquid phase was completely degraded. Few products (such as 9-phenanthenol) were detected in the solid phase, and the main products in the liquid phase were 2,4-di-*tert*-butylphenol and diphenaldehyde. The changes of peak areas of these products are shown in Fig. S4. The peak areas of 9-phenanthenol and diphenaldehyde have the maximum values at 1 min and 3 min respectively, while the peak areas of 2,4-di-*tert*-butylphenol increase with the increase of time. During the entire degradation process (1-30 min), no chlorinated byproducts were detected. There are two possible explanations for this: 1) after ·Cl reacted with the benzene ring (free radical addition), the resultant compound reacted with water molecules to remove HCl and formed a hydroxyl compound (Martire et al., 2001); and 2) the chlorination byproducts were degraded by ·OH very rapidly. Overall, Phe in the Fenton/Cl^- system can be degraded by ·Cl and a large number of chlorinated byproducts will not be formed.

The acute and chronic toxicity of Phe and its products were calculated by ECOSAR software (Table S3) (Liang et al., 2019). 2,4-di-*tert*-butylphenol is the only degradation product with higher toxicity than Phe. 2,4-di-*tert*-butylphenol was not detected in other related studies on degradation of Phe (Table S4) (Bendouz et al., 2017; Gu et al., 2018; Woo et al., 2009). Therefore, the appearance of 2,4-di-*tert*-butylphenol is probably due to the action of Cl^-. In this study, 2,4-di-*tert*-butylphenol (hydrophobic compound) only appeared in the liquid phase, and its content increased with the increase of reaction time. This is probably because Phe was degraded into hydrophilic compounds during Fenton/Cl^- treatment, and then the hydrophilic compounds (such as phenol) reacted with small molecular compounds (such as alcohols and olefins) in liquid phase by Friedel-Grafts reaction under the catalysis of $FeCl_3$ to form 2,4-di-*tert*-butylphenol (Zhu, 2011). Therefore, the formation of toxic products is not due to free radical RCS, but to the catalytic action of $FeCl_3$; the formation of 2,4-di-*tert*-butylphenol is inevitable when the iron-based system is used to treat chlorine-containing wastewater or sludge. Generally speaking, the sludge conditioned by iron-based system is incinerated, and the sewage of sludge is returned to the wastewater plant for treatment, which may be a friendlier disposal method than sludge landfill and reuse.

Fenton, a classical AOP, is widely used (Zhang et al., 2019a). There are two speed-limiting steps for Fenton/Cl^- system to degrade trace organic pollutants in sludge: 1) reduction of Fe^{3+} in the Fenton system ($Fe^{3+} + H_2O_2 \rightarrow Fe^{2+} + HO_2^{\cdot} + H^+$) (Zhu et al., 2019); 2) contact between reactive species in liquid phase and PAHs in solid phase (Lin et al., 2016). Therefore, how to speed up the redox cycle of Fe(III)/Fe(II) and improve the utilization efficiency of H_2O_2 in Fenton reaction is the core issue studied by many scholars (Zhu et al., 2019). However, researches on Fenton and Fenton-like systems mainly focus on the formation of ·OH, the circulation of Fe^{2+}/Fe^{3+} (Zhu et al., 2019) and the interference of inorganic ions (Ribeiro et al., 2019), while ignoring the action of RCS, the formation of chlorination byproducts and toxic products. In addition, conditioning and disposal (incineration, agricultural reuse and landfill) are often considered separately in the whole process of sludge treatment and disposal. In this investigation, Fenton/Cl^- system was used for treating PAHs in simulated sludge, and the role of RCS and the risk of conditioning were explored. It was proved that Fenton may be used as a clean technology to treat PAHs in TDS on the premise of incineration. However, resulting from the complex composition of TDS, many organic compounds except PAHs may be chlorinated by free-radical RCS in the Fenton/Cl^- system, so the formation of chlorination byproducts in actual TDS still needs further study.

4. Conclusion

For exploring the potential hidden trouble of the Fenton system in sludge treatment, PAHs in simulated sludge were degraded by the Fenton/Cl^- system in this study. The [·OH]$_{ss}$, [·Cl]$_{ss}$, and [$Cl_2^{\cdot-}$]$_{ss}$ in the complex system were determined using TBA, NB, and BA for the first time. It was found that the concentration of reactive species (·OH, ·Cl, $Cl_2^{\cdot-}$, and $HO_2^{\cdot}$/$O_2^{\cdot-}$) and the removal of PAHs changed regularly with changes in Cl^- concentration and pH value. The increase of Cl^- and pH was not necessarily unfavorable to the removal of PAHs. Comprehensive results showed that ·Cl in the Fenton/Cl^- system had strong reactivity with Phe, while the weak reactivity of $Cl_2^{\cdot-}$ with PAHs could be ignored. $HO_2^{\cdot}$/$O_2^{\cdot-}$ was helpful in removing Ant and Flu from the solid phase of simulated sludge. On the premise of high Cl^- content (≥1000 mg/L), PAHs could be removed more effectively by using $HO_2^{\cdot}$/$O_2^{\cdot-}$ in micro-acid environment. In this study, the reactivity of reactive species (·Cl, $Cl_2^{\cdot-}$, and $HO_2^{\cdot}$/$O_2^{\cdot-}$) and multi-structure PAHs was clearly recognized, which provided a basis for further investigations on the efficient degradation of target organic compounds in the Fenton/Cl^- system. In addition, according to the product analysis of Phe, it was found that the addition reaction of ·Cl in the Fenton/Cl^- system would not produce chlorination byproducts and the solid-phase toxicity of the treated sludge would be weakened. Therefore, on the premise of incineration, Fenton system interfered by Cl^- may still be a reliable clean technology for PAHs degradation.

Acknowledgments

The authors thank the support of the Local Innovative and Research Teams Project of Guangdong Pearl River Talents Program [Grant No. 2017BT01Z032], the 2017 Central Special Fund for Soil, Preliminary Study on Harmless Treatment and Comprehensive Utilization of Tailings in Dabao Mountain [18HK0108], and the National Natural Science Foundation of China [Grant No. 21577027].

References

Alegre, M.L., Gerones, M., Rosso, J.A., Bertolotti, S.G., Braun, A.M., Martire, D.O., Gonzalez, M.C., 2000. Kinetic study of the reactions of chlorine atoms and $Cl_2^{\cdot -}$ radical anions in aqueous solutions. 1. Reaction with benzene. J. Phys. Chem. A 104, 3117-3125.

Bataineh, H., Pestovsky, O., Bakac, A., 2012. pH-induced mechanistic changeover from hydroxyl radicals to iron(IV) in the Fenton reaction. Chem. Sci. 3, 1594-1599.

Beitz, T., Bechmann, W., Mitzner, R., 1998. Investigations of reactions of selected azaarenes with radicals in water. 2. Chlorine and bromine radicals. J. Phys. Chem. A 102, 6766-6771.

Bendouz, M., Tran, L.H., Coudert, L., Mercier, G., Blais, J.F., 2017. Degradation of polycyclic aromatic hydrocarbons in different synthetic solutions by Fenton's oxidation. Environ. Technol. 38, 116-127.

Chen, N., Huang, Y.H., Hou, X.J., Ai, Z.H., Zhang, L.Z., 2017. Photochemistry of

Hydrochar: Reactive Oxygen Species Generation and Sulfadimidine Degradation. Environ. Sci. Technol. 51, 11278-11287.

Crump, B., Ernst, W.R., Neumann, H.M., 1998. Influence of H_2O_2 on a chloride-dependent reaction path to chlorine dioxide. AICHE J. 44, 2494-2500.

Fang, J.Y., Fu, Y., Shang, C., 2014. The Roles of Reactive Species in Micropollutant Degradation in the UV/Free Chlorine System. Environ. Sci. Technol. 48, 1859-1868.

Flotron, V., Delteil, C., Padellec, Y., Camel, V., 2005. Removal of sorbed polycyclic aromatic hydrocarbons from soil, sludge and sediment samples using the Fenton's reagent process. Chemosphere 59, 1427-1437.

Gu, M.B., Sui, Q., Farooq, U., Zhang, X., Qiu, Z.F., Lyu, S.G., 2018. Degradation of phenanthrene in sulfate radical based oxidative environment by nZVI-PDA functionalized rGO catalyst. Chem. Eng. J. 354, 541-552.

Guan, R.P., Yuan, X.Z., Wu, Z.B., Jiang, L.B., Li, Y.F., Zeng, G.M., 2018. Principle and application of hydrogen peroxide based advanced oxidation processes in activated sludge treatment: A review. Chem. Eng. J. 339, 519-530.

Guo, K.H., Wu, Z.H., Shang, C., Yao, B., Hou, S.D., Yang, X., Song, W.H., Fang, J.Y., 2017. Radical Chemistry and Structural Relationships of PPCP Degradation by UV/Chlorine Treatment in Simulated Drinking Water. Environ. Sci. Technol. 51, 10431-10439.

Hasegawa, K., Neta, P., 1978. Rate constants and mechanisms of reaction of $Cl_2^{\cdot -}$ radicals. J. Phys. Chem. 82, 854-857.

He, J., Yang, X.F., Men, B., Wang, D.S., 2016. Interfacial mechanisms of heterogeneous Fenton reactions catalyzed by iron-based materials: A review. J. Environ. Sci.-China 39, 97-109.

Hu, Y., Zhang, C., Wang, D.Z., Wen, J.Y., Chen, M.H., Li, Y., 2013. Chloride ion transport and fate in oilfield wastewater reuse by interval dynamic multimedia aquivalence model. Water Sci. Technol. 67, 628-634.

Hua, Z.C., Guo, K.H., Kong, X.J., Lin, S.K., Wu, Z.H., Wang, L.P., Huang, H., Fang, J.Y., 2019. PPCP degradation and DBP formation in the solar/free chlorine system: Effects of pH and dissolved oxygen. Water Res. 150, 77-85.

Huang, Y., Sheng, B., Wang, Z.H., Liu, Q.Z., Yuan, R.X., Xiao, D.X., Liu, J.S., 2018. Deciphering the degradation/chlorination mechanisms of maleic acid in the Fe(II)/peroxymonosulfate process: An often overlooked effect of chloride. Water Res. 145, 453-463.

Jia, H.Z., Zhao, S., Zhu, K.C., Huang, D., Wu, L., Guo, X.T., 2018. Activate persulfate for catalytic degradation of adsorbed anthracene on coking residues: Role of persistent free radicals. Chem. Eng. J. 351, 631-640.

Jung, Y.S., Lim, W.T., Park, J.Y., Kim, Y.H., 2009. Effect of pH on Fenton and Fenton-like oxidation. Environ. Technol. 30, 183-190.

Karunanayake, A.G., Todd, O.A., Crowley, M.L., Ricchetti, L.B., Pittman, C.U., Anderson, R., Mlsna, T.E., 2017. Rapid removal of salicylic acid, 4-nitroaniline, benzoic acid and phthalic acid from wastewater using magnetized fast pyrolysis biochar from waste

Douglas fir. Chem. Eng. J. 319, 75-88.

Ke, Y.W., Ning, X.A., Liang, J.Y., Zou, H.Y., Sun, J., Cai, H.L., Lin, M.Q., Li, R.J., Zhang, Y.P., 2018. Sludge treatment by integrated ultrasound-Fenton process: Characterization of sludge organic matter and its impact on PAHs removal. J. Hazard. Mater. 343, 191-199.

Krizanec, B., Le Marechal, A.M., 2006. Dioxins and dioxin-like persistent organic pollutants in textiles and chemicals in the textile sector. Croat. Chem. Acta 79, 177-186.

Lai, X.J., Ning, X.A., Chen, J.Y., Li, Y., Zhang, Y.P., Yuan, Y.Q., 2020. Comparison of the Fe^{2+}/H_2O_2 and Fe^{2+}/PMS systems in simulated sludge: Removal of PAHs, migration of elements and formation of chlorination byproducts. J. Hazard. Mater. 398, 122826.

Lai, X.J., Ning, X.A., He, Y., Yuan, Y.Q., Sun, J., Ke, Y.W., Man, X.Y., 2019. Treatment of a simulated sludge by ultrasonic zero-valent iron/EDTA/Air process: Interferences of inorganic salts in polyaromatic hydrocarbon removal. Waste Manage. 85, 548-556.

Lee, B.D., Iso, M., Hosomi, M., 2001. Prediction of Fenton oxidation positions in polycyclic aromatic hydrocarbons by Frontier electron density. Chemosphere 42, 431-435.

Lei, Y., Lei, X., Westerhoff, P., Zhang, X., Yang, X., 2021. Reactivity of Chlorine Radicals ($\cdot$Cl and $Cl_2^{\cdot-}$)) with Dissolved Organic Matter and the Formation of Chlorinated Byproducts. Environ. Sci. Technol. 55, 689-699.

Li, X.W., Liu, X.T., Lin, C.Y., Zhou, Z., He, M.C., Ouyang, W., 2020. Catalytic oxidation of contaminants by Fe^0 activated peroxymonosulfate process: Fe(IV) involvement, degradation intermediates and toxicity evaluation. Chem. Eng. J. 382, 123013.

Liang, J.Y., Ning, X.A., Lai, X.J., Zou, H.Y., Sun, J., Lu, X.W., Zhang, Y.P., An, T.C., 2017. Influence mechanisms of textile-dyeing sludge characteristics on degradation of anilines by integrated ultrasound-permanganate treatment. J. Clean Prod. 151, 172-178.

Liang, J.Y., Ning, X.A., Song, J., Lu, X.W., Sun, J., Zhang, Y.P., 2019. Treatment of 3,3 '-dimethoxybenzidine in sludge by advance oxidation process: Degradation products and toxicity evaluation. J. Environ. Manage. 238, 102-109.

Liang, X., Ning, X.A., Chen, G.X., Lin, M.Q., Liu, J.Y., Wang, Y.J., 2013. Concentrations and speciation of heavy metals in sludge from nine textile dyeing plants. Ecotoxicol. Environ. Saf. 98, 128-134.

Lin, M.Q., Ning, X.A., An, T.C., Zhang, J.H., Chen, C.M., Ke, Y.W., Wang, Y.J., Zhang, Y.P., Sun, J., Liu, J.Y., 2016. Degradation of polycyclic aromatic hydrocarbons (PAHs) in textile dyeing sludge with ultrasound and Fenton processes: Effect of system parameters and synergistic effect study. J. Hazard. Mater. 307, 7-16.

Lu, M.C., Chang, Y.F., Chen, I.M., Huang, Y.Y., 2005. Effect of chloride ions on the oxidation of aniline by Fenton's reagent. J. Environ. Manage. 75, 177-182.

Ma, W.J., Wang, N., Du, Y.C., Tong, T.Z., Zhang, L.J., Lin, K.Y.A., Han, X.J., 2019. One-step synthesis of novel Fe_3C@nitrogen-doped carbon nanotubes/graphene nanosheets for catalytic degradation of Bisphenol A in the presence of peroxymonosulfate. Chem. Eng. J. 356, 1022-1031.

Martire, D.O., Rosso, J.A., Bertolotti, S., Le Roux, G.C., Braun, A.M., Gonzalez, M.C., 2001. Kinetic study of the reactions of chlorine atoms and $Cl_2^{\bullet-}$ radical anions in aqueous solutions. II. Toluene, benzoic acid, and chlorobenzene. J. Phys. Chem. A 105, 5385-5392.

Meghlaoui, F.Z., Merouani, S., Hamdaoui, O., Bouhelassa, M., Ashokkumar, M., 2019. Rapid catalytic degradation of refractory textile dyes in Fe(II)/chlorine system at near neutral pH: Radical mechanism involving chlorine radical anion ($Cl_2^{\bullet-}$)-mediated transformation pathways and impact of environmental matrices. Sep. Purif. Technol. 227,115685.

NDRL/NIST, 2017. National institute of standards and technology, NDRL/NIST solution kinetcis database on the web. http://www3.nd.edu/ndrlrcdc/index.html (Accessed November 20, 2017).

Nganai, S., Lomnicki, S., Dellinger, B., 2009. Ferric Oxide Mediated Formation of PCDD/Fs from 2-Monochlorophenol. Environ. Sci. Technol. 43, 368-373.

Nikravesh, B., Shomalnasab, A., Nayyer, A., Aghababaei, N., Zarebi, R., Ghanbari, F., 2020. UV/Chlorine process for dye degradation in aqueous solution: Mechanism, affecting factors and toxicity evaluation for textile wastewater. J. Environ. Chem. Eng. 8, 104244.

Ning, X.A., Liang, J.Y., Li, R.J., Hong, Z., Wang, Y.J., Chang, K.L., Zhang, Y.P., Yang, Z.Y., 2015. Aromatic amine contents, component distributions and risk assessment in sludge from 10 textile-dyeing plants. Chemosphere 134, 367-373.

Ning, X.A., Lin, M.Q., Shen, L.Z., Zhang, J.H., Wang, J.Y., Wang, Y.J., Yang, Z.Y., Liu, J.Y., 2014. Levels, composition profiles and risk assessment of polycyclic aromatic hydrocarbons (PAHs) in sludge from ten textile dyeing plants. Environ. Res. 132, 112-118.

Raheem, A., Sikarwar, V.S., He, J., Dastyar, W., Dionysiou, D.D., Wang, W., Zhao, M., 2018. Opportunities and challenges in sustainable treatment and resource reuse of sewage sludge: A review. Chem. Eng. J. 337, 616-641.

Ribeiro, A.R.L., Moreira, N.F.F., Puma, G.L., Silva, A.M.T., 2019. Impact of water matrix on the removal of micropollutants by advanced oxidation technologies. Chem. Eng. J. 363, 155-173.

Sanchez-Brunete, C., Miguel, E., Tadeo, J.L., 2007. Analysis of 27 polycyclic aromatic hydrocarbons by matrix solid-phase dispersion and isotope dilution gas chromatography-mass spectrometry in sewage sludge from the Spanish area of Madrid. J. Chromatogr. A 1148, 219-227.

Smith, B.A., Teel, A.L., Watts, R.J., 2006. Mechanism for the destruction of carbon tetrachloride and chloroform DNAPLs by modified Fenton's reagent. J. Contam. Hydrol. 85, 229-246.

Smith, B.A., Teel, A.L., Watts, R.J., 2015. Destruction of 1,1,1-trichloroethane and 1,2-dichloroethane DNAPLs by catalyzed H_2O_2 propagations (CHP). J. Environ. Sci. Heal. A 50, 846-854.

Sun, H.W., Yan, Q.S., 2008. Influence of pyrene combination state in soils on its treatment efficiency by Fenton oxidation. J. Environ. Manage. 88, 556-563.

Varanasi, L., Coscarelli, E., Khaksari, M., Mazzoleni, L.R., Minakata, D., 2018. Transformations of dissolved organic matter induced by UV photolysis, Hydroxyl radicals, chlorine radicals, and sulfate radicals in aqueous-phase UV-Based advanced oxidation processes. Water Res. 135, 22-30.

Wang, M.H., Xu, L., 2003. General Chemistry. Higher Education Press, Beijing.

Wang, T.J., Chen, T., Lin, B.B., Lin, X.Q., Zhan, M.X., Li, X.D., 2017. Emission characteristics and relationships among PCDD/Fs, chlorobenzenes, chlorophenols and PAHs in the stack gas from two municipal solid waste incinerators in China. Rsc. Adv. 7, 44309-44318.

Wang, Z., Qiu, W., Pang, S.Y., Gao, Y., Zhou, Y., Cao, Y., Jiang, J., 2020. Relative contribution of ferryl ion species (Fe(IV)) and sulfate radical formed in nanoscale zero valent iron activated peroxydisulfate and peroxymonosulfate processes. Water Res. 172, 115504.

Wang, Z., Qiu, W., Pang, S.Y., Jiang, J., 2019. Effect of chelators on the production and nature of the reactive intermediates formed in Fe(II) activated peroxydisulfate and hydrogen peroxide processes. Water Res. 164, 114957.

Watts, R.J., Teel, A.L., 2019. Hydroxyl radical and non-hydroxyl radical pathways for trichloroethylene and perchloroethylene degradation in catalyzed H_2O_2 propagation systems. Water Res. 159, 46-54.

Weng, H.X., Ji, Z.Q., Chu, Y., Cheng, C.Q., Zhang, J.J., 2012. Benzene series in sewage sludge from China and its release characteristics during drying process. Environ. Earth. Sci. 65, 561-569.

Woo, O.T., Chung, W.K., Wong, K.H., Chow, A.T., Wong, P.K., 2009. Photocatalytic oxidation of polycyclic aromatic hydrocarbons: Intermediates identification and toxicity testing. J. Hazard. Mater. 168, 1192-1199.

Wu, Y.X., Yang, Y., Liu, Y.Z., Zhang, L.Q., Feng, L., 2019. Modelling study on the effects of chloride on the degradation of bezafibrate and carbamazepine in sulfate radical-based advanced oxidation processes: Conversion of reactive radicals. Chem. Eng. J. 358, 1332-1341.

Wu, Z.H., Fang, J.Y., Xiang, Y.Y., Shang, C., Li, X.C., Meng, F.G., Yang, X., 2016. Roles of reactive chlorine species in trimethoprim degradation in the UV/chlorine process: Kinetics and transformation pathways. Water Res. 104, 272-282.

Xu, T.Y., Zhu, R.L., Zhu, G.Q., Zhu, J.X., Liang, X.L., Zhu, Y.P., He, H.P., 2017. Mechanisms for the enhanced photo-Fenton activity of ferrihydrite modified with $BiVO_4$ at neutral pH. Appl. Catal., B-Environ. 212, 50-58.

Yuan, R.X., Ramjaun, S.N., Wang, Z.H., Liu, J.S., 2011. Effects of chloride ion on degradation of Acid Orange 7 by sulfate radical-based advanced oxidation process: Implications for formation of chlorinated aromatic compounds. J. Hazard. Mater. 196, 173-179.

Zhang, M.H., Dong, H., Zhao, L., Wang, D.X., Meng, D., 2019a. A review on Fenton process for organic wastewater treatment based on optimization perspective. Sci. Total Environ. 670, 110-121.

Zhang, X.Y., Yu, T., Li, X., Yao, J.Q., Liu, W.G., Chang, S.L., Chen, Y.G., 2019b. The fate and enhanced removal of polycyclic aromatic hydrocarbons in wastewater and sludge treatment system: A review. Crit. Rev. Env. Sci. Tec. 49, 1425-1475.

Zhou, X., Zhou, Y.X., Liu, J.S., Song, S., Sun, J.J., Zhu, G.H., Gong, H.P., Wang, L., Wu, C.W., Li, M.F., 2019. Study on the pollution characteristics and emission factors of PCDD/Fs from disperse dye production in China. Chemosphere 228, 328-334.

Zhu, B.C., 2011. Chemical reaction engineering, 5th edition. Chemical Industry Press, China.

Zhu, Y.P., Zhu, R.L., Xi, Y.F., Zhu, J.X., Zhu, G.Q., He, H.P., 2019. Strategies for enhancing the heterogeneous Fenton catalytic reactivity: A review. Appl. Catal., B-Environ. 255, 117739.

Zou, H.Y., Ning, X.A., Wang, Y., Zhou, F.P., 2019. The agricultural use potential of the detoxified textile dyeing sludge by integrated Ultrasound/Fenton-like process: A comparative study. Ecotoxicol. Environ. Saf. 172, 26-32.

Table captions

Table 1 Organic matter and heavy metals in the textile dyeing sludge.

Table 2 Outcomes of the first-order rate constants of PAHs (Phe, Ant, and Flu) removal from the simulated sludge solid phase by the Fenton/Cl^- system between 5 and 30 minutes.

Table 3 Second-order rate constants of homogeneous reaction of organic compounds (scavengers or probes) with $\cdot OH$, $\cdot Cl$, $Cl_2^{\cdot -}$ or $HO_2^{\cdot}/O_2^{\cdot -}$ in aqueous phase without catalyst.

Figure captions

Fig. 1 Effect of the Cl^- content on the PAHs ((a) Phe, (b) Ant, (c) Flu, and (d) $\sum_3$PAHs) removal from the simulated sludge solid phase by the Fenton/Cl^- system (Fenton/Cl^- conditions: pH=3.0, $H_2O_2/Fe^{2+}=1/1$, $H_2O_2=30$ mM, 40 min).

Fig. 2 Effect of pH on the PAHs ((a) Phe, (b) Ant, (c) Flu, and (d) $\sum_3$PAHs) removal from the simulated sludge solid phase by the Fenton/Cl^- system (Fenton/Cl^- conditions: $H_2O_2/Fe^{2+}=1/1$, $H_2O_2=30$ mM, Cl^- =1000 mg/L, 40 min).

Fig. 3 The contribution of free radicals to PAHs ((a) Phe, (b) Ant, and (c) Flu) removal from simulated sludge solid phase (Fenton/Cl^- conditions: $H_2O_2/Fe^{2+}=1/1$, $H_2O_2=30$ mM, 40 min).

Fig. 4 EPR spectra of DMPO-OOH adduct formed after 3 min in the Fenton/Cl^- system (Fenton/Cl^- conditions: $H_2O_2/Fe^{2+}=1/1$, $H_2O_2=30$ mM, 25 □).

Fig. 5 Effect of pH on the adsorption of free-radical probes (NB, BA, and TBA) by the solid phase of simulated sludge and the first-order rate constants of simulated sludge solid phase adsorption.

Fig. 6 Effects of (a) Cl^- concentration and (b) pH on the steady-state concentration of free radicals (·OH, ·Cl, and $Cl_2^{\cdot -}$) in the Fenton/Cl^- system.

Table 1 Organic matter and heavy metals in the textile dyeing sludge.

Pollutants	Concentration	Threshold values (Environmental Protection Administration, PR China)	
		Agricultural sludge (GB 4284-2018, A grade)	Sludge burned separately (GB/T 24602-2009)
Cu (mg/kg DS)	61.5 – 571 [a,b]	500	100
Pb (mg/kg DS)	6.32 – 36.9 [a,b]	3	5
Ni (mg/kg DS)	31.5 – 193 [a,b]	100	5
Cd (mg/kg DS)	1.16 – 5.66 [a,b]	500	15
Cr (mg/kg DS)	69.2 – 577 [a,b]	3	1
Zn (mg/kg DS)	42.5 – 2585 [a,b]	1200	100
Mono-benzene compound (mg/kg DS)	12.81 – 54.97 [c]	–	–
Anilines (mg/kg DS)	11.0 – 82.5 [b,d,e]	–	–
Dioxins	1.72 – 657 ng I-TEQ/kg [f,g]	–	1.0 ng TEQ/m^3
Σ_{16} PAHs (mg/kg DS)	1.46 – 16.71 [h]	5	–

[a] (Liang et al., 2013); [b] (Zou et al., 2019); [c] (Weng et al., 2012); [d] (Ning et al., 2015); [e] (Liang et al., 2017); [f] (Krizanec and Le Marechal, 2006); [g] (Zhou et al., 2019); [h] (Ning et al., 2014).

Table 2 Outcomes of the first-order rate constants of PAHs (Phe, Ant, and Flu) removal from the simulated sludge solid phase by the Fenton/Cl^- system between 5 and 30 minutes.

pH	Cl^- (mg/L)	First-order rate constants (/s)			
		Phe	Ant	Flu	$\sum_3$ PAHs
3.0	50	2.77×10^{-4} (R^2 = 0.99)	9.63×10^{-4} (R^2 = 0.95)	5.40×10^{-4} (R^2 = 0.91)	6.42×10^{-4} (R^2 = 0.95)
	100	1.86×10^{-4} (R^2 = 0.75)	7.16×10^{-4} (R^2 = 0.97)	1.69×10^{-4} (R^2 = 0.99)	4.10×10^{-4} (R^2 = 0.99)
	500	2.14×10^{-4} (R^2 = 0.94)	3.96×10^{-4} (R^2 = 0.85)	3.03×10^{-4} (R^2 = 0.98)	3.33×10^{-4} (R^2 = 0.96)
	1000	7.75×10^{-4} (R^2 = 0.92)	4.06×10^{-4} (R^2 = 0.78)	6.17×10^{-4} (R^2 = 0.94)	5.44×10^{-4} (R^2 = 0.90)
	2000	4.10×10^{-4} (R^2 = 0.89)	3.28×10^{-4} (R^2 = 0.86)	4.79×10^{-4} (R^2 = 0.77)	4.11×10^{-4} (R^2 = 0.88)
4.0	1000	1.51×10^{-4} (R^2 = 0.99)	4.23×10^{-4} (R^2 = 0.91)	1.57×10^{-4} (R^2 = 0.96)	2.00×10^{-4} (R^2 = 0.97)
5.0	1000	1.32×10^{-4} (R^2 = 0.10)	4.15×10^{-4} (R^2 = 0.80)	0.88×10^{-4} (R^2 = 0.78)	1.24×10^{-4} (R^2 = 0.88)

Table 3 Second-order rate constants of homogeneous reaction of organic compounds (scavengers or probes) with ·OH, ·Cl, $Cl_2^{\cdot -}$ or $HO_2^{\cdot}/O_2^{\cdot -}$ in aqueous phase without catalyst.

Reaction		Rate constants (/Ms)	Conditions	References
Scavenger or probe	Reactive species			
BQ	·OH	1.2×10^{9}	25 □, pH=7.0	(NDRL/NIST, 2017)
	·Cl	UN	UN	UN
	$Cl_2^{\cdot -}$	UN	UN	UN
	$HO_2^{\cdot}/O_2^{\cdot -}$	9.6×10^{8}	25 □, pH=7.0	(He et al., 2016)
NB	·OH	3.9×10^{9}	25 □, pH=2.0-9.0	(Fang et al., 2014)
	·Cl	N	25 □, pH=2.0-9.0	(Fang et al., 2014)
	$Cl_2^{\cdot -}$	N	25 □, pH=2.0-9.0	(Fang et al., 2014)
	$HO_2^{\cdot}/O_2^{\cdot -}$	N	20±2 □, pH=3.0	(Watts and Teel, 2019)
TBA	·OH	6.0×10^{8}	25 □, pH=3.0-9.0	(Li et al., 2020)
	·Cl	3.0×10^{8}	25 □, pH=2.0	(NDRL/NIST, 2017)
	$Cl_2^{\cdot -}$	7.0×10^{2}	25 □, pH=1.0	(Hasegawa and Neta, 1978)
	$HO_2^{\cdot}/O_2^{\cdot -}$	N	25 □, pH=2.0-8.0	(Ma et al., 2019)
BA	·OH	5.9×10^{9}	25±2 □, pH=3.0-8.0	(Hua et al., 2019; Varanasi et al., 2018)
	·Cl	1.8×10^{10}	25±2 □, pH=3.0-8.0	(Hua et al., 2019; Varanasi et al., 2018)
	$Cl_2^{\cdot -}$	2.0×10^{6}	25 □, pH=7.0	(Hasegawa and Neta, 1978)
	$HO_2^{\cdot}/O_2^{\cdot -}$	N	25 □, pH=2.0-8.0	(Ma et al., 2019)

N: negligible; UN: unknown.

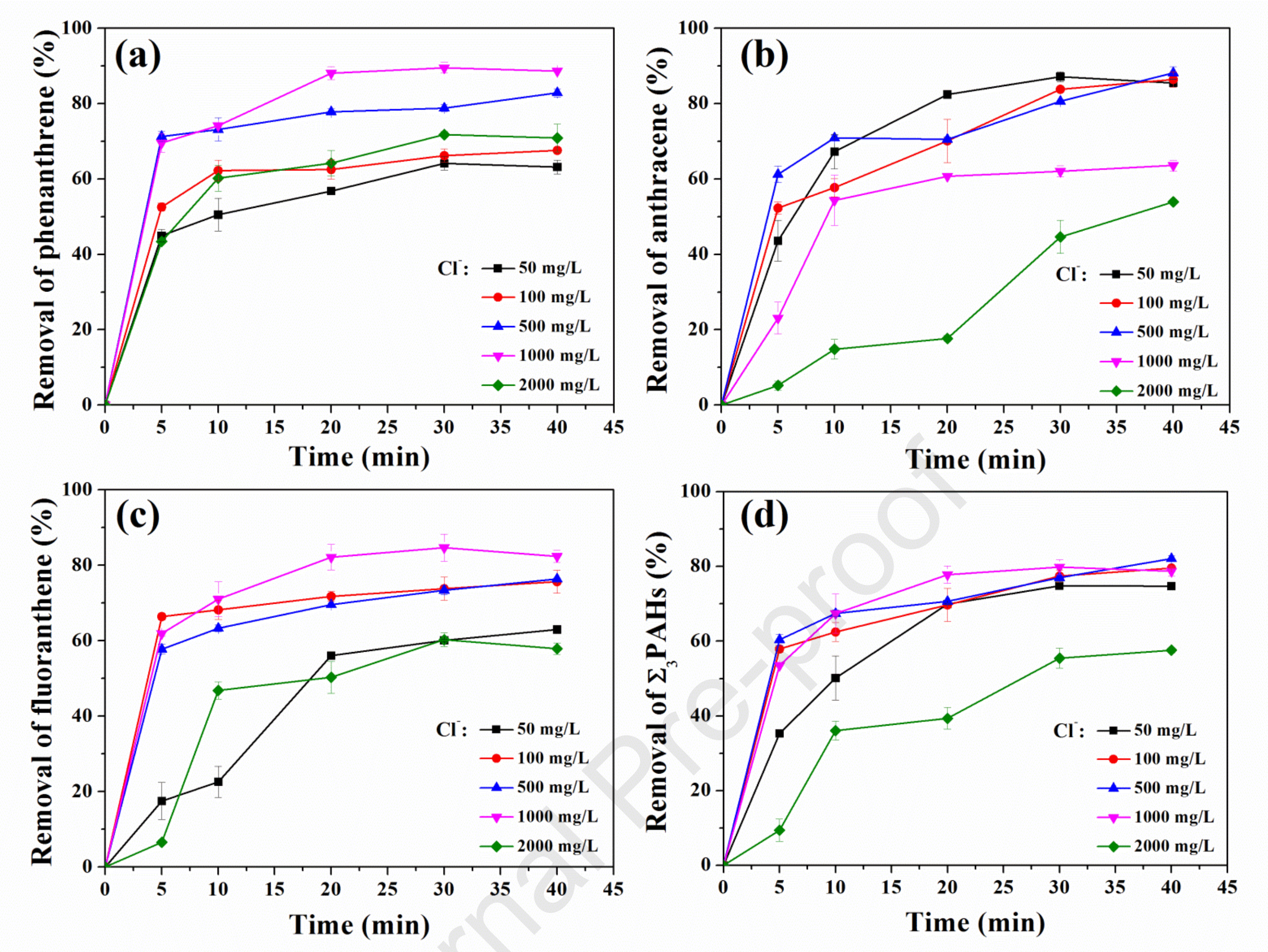

Fig. 1 Effect of the Cl$^-$ content on the PAHs ((a) Phe, (b) Ant, (c) Flu, and (d) $\sum_3$PAHs) removal from the simulated sludge solid phase by the Fenton/Cl$^-$ system (Fenton/Cl$^-$ conditions: pH=3.0, H_2O_2/Fe^{2+}=1/1, H_2O_2=30 mM, 40 min).

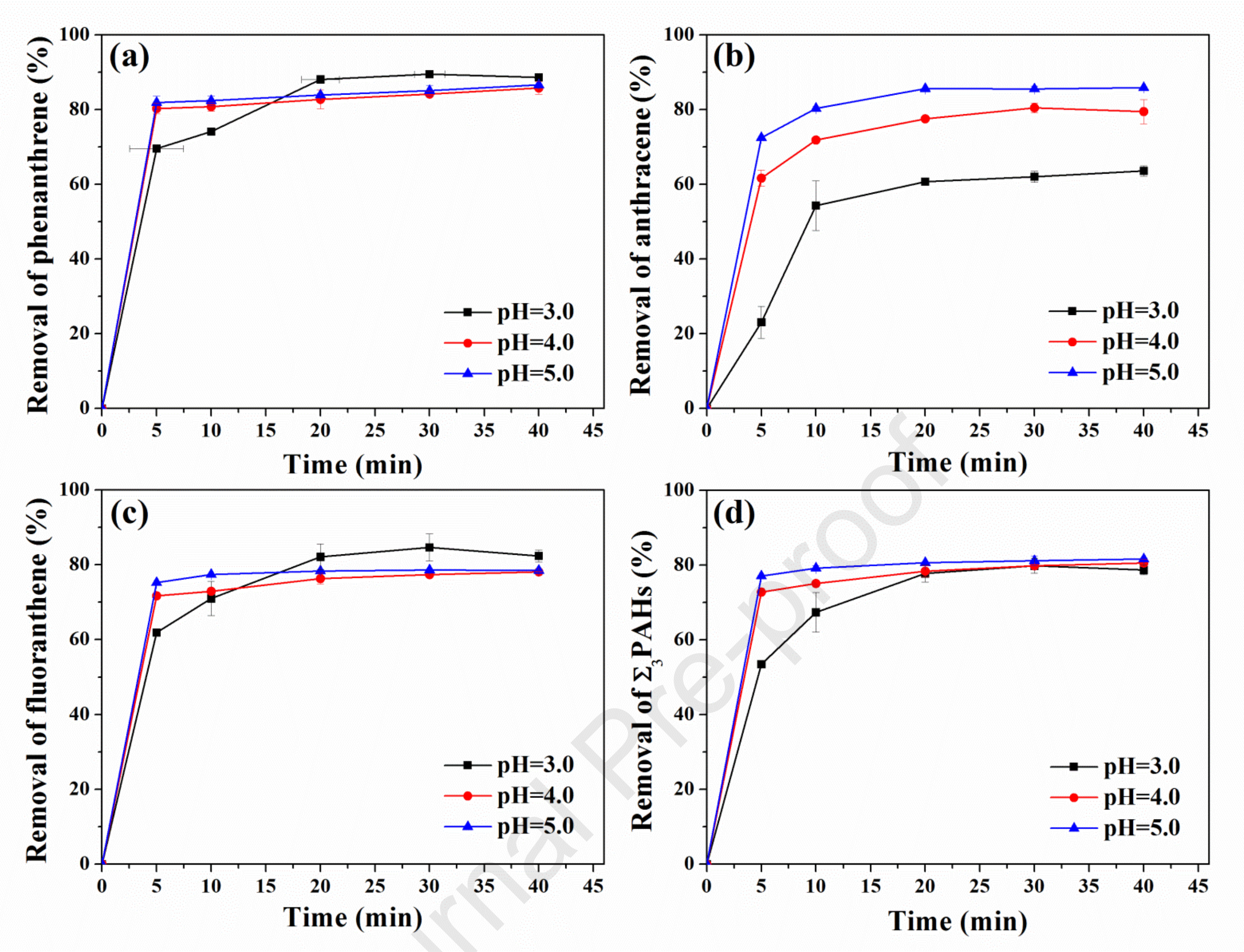

Fig. 2 Effect of pH on the PAHs ((a) Phe, (b) Ant, (c) Flu, and (d) $\sum_3$PAHs) removal from the simulated sludge solid phase by the Fenton/Cl^- system (Fenton/Cl^- conditions: H_2O_2/Fe^{2+}=1/1, H_2O_2=30 mM, Cl^- =1000 mg/L, 40 min).

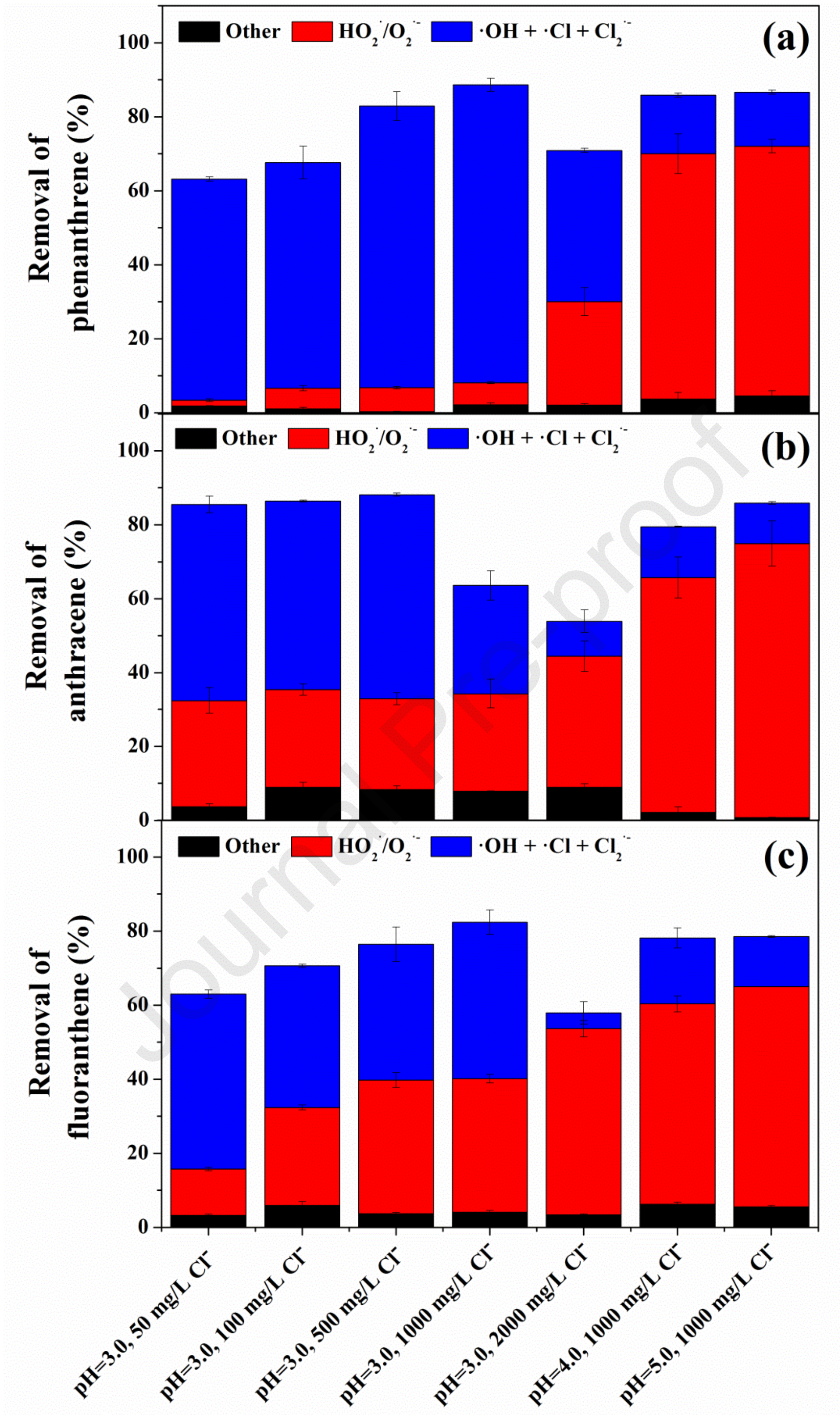

Fig. 3 The contribution of free radicals to PAHs ((a) Phe, (b) Ant, and (c) Flu) removal from simulated sludge solid phase (Fenton/Cl$^-$ conditions: H_2O_2/Fe^{2+}=1/1, H_2O_2=30 mM, 40 min).

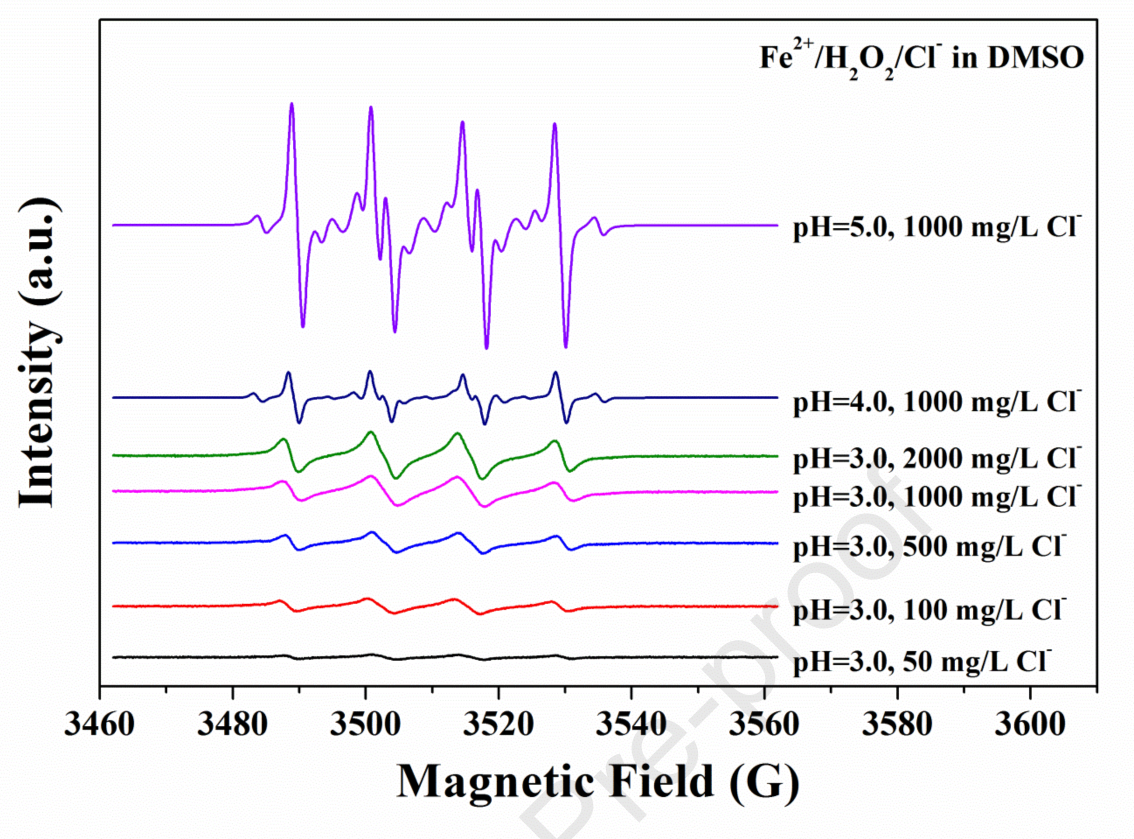

Fig. 4 EPR spectra of DMPO-OOH adduct formed after 3 min in the Fenton/Cl^- system (Fenton/Cl^- conditions: H_2O_2/Fe^{2+}=1/1, H_2O_2=30 mM, 25 □).

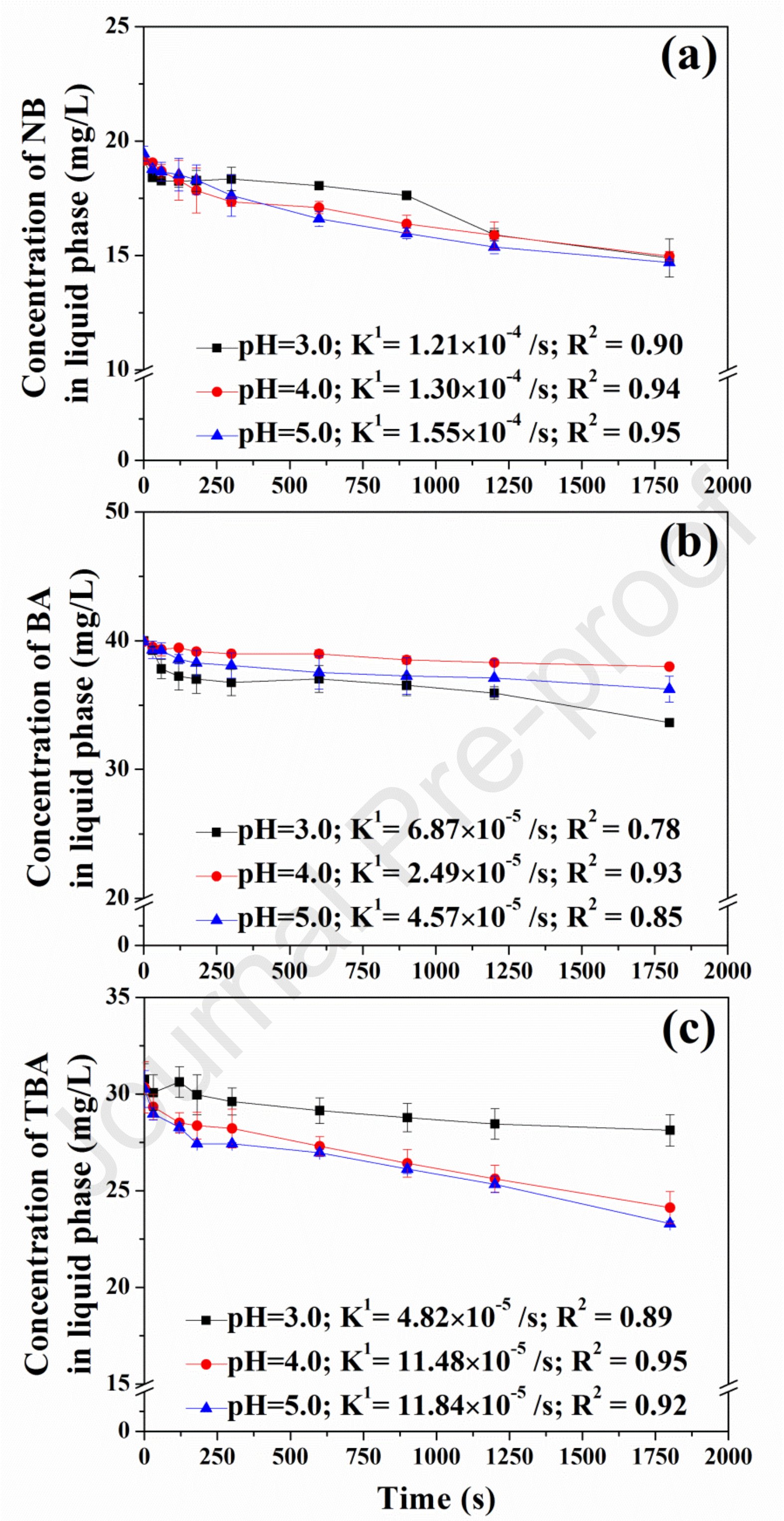

Fig. 5 Effect of pH on the adsorption of free-radical probes (NB, BA, and TBA) by the solid phase of simulated sludge and the first-order rate constants of simulated sludge solid phase adsorption.

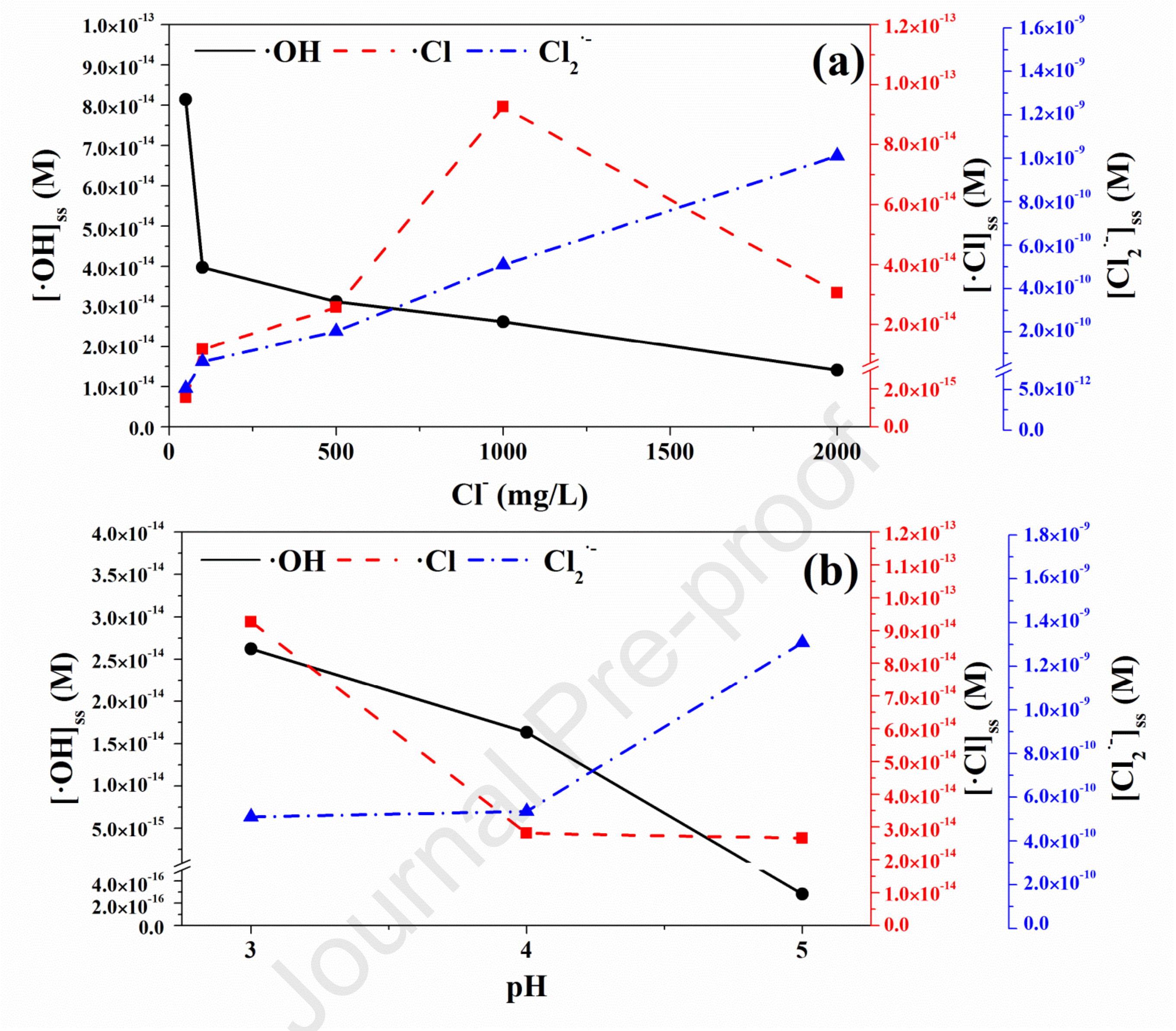

Fig. 6 Effects of (a) Cl^- concentration and (b) pH on the steady-state concentration of free radicals (·OH, ·Cl, and $Cl_2^{\cdot -}$) in the Fenton/Cl^- system.

Highlights

- $[\cdot OH]_{ss}$, $[\cdot Cl]_{ss}$, and $[Cl_2^{\cdot -}]_{ss}$ were determined using TBA, NB, and BA
- $\cdot$Cl (9.27×10^{-14} M, MAX) in Fenton/Cl^- enhanced Phe removal without forming chloride
- $HO_2^{\cdot}/O_2^{\cdot -}$ in Fenton/Cl^- was increased by increasing Cl^- concentration or pH
- The reactivity of $HO_2^{\cdot}/O_2^{\cdot -}$ is greater with Ant and Flu than with Phe

Supporting Information for

Treatment of simulated textile sludge using the Fenton/Cl^- system: the roles of chlorine radicals and superoxide anions on PAHs removal

Xiaojun Lai, Xun-an Ning*, Yaping Zhang, Yang Li, Riwen Li, Jiayi Chen, Shiyin Wu

Guangdong Key Laboratory of Environmental Catalysis and Health Risk Control, Institute of Environmental Health and Pollution Control, School of Environmental Science and Engineering, Guangdong University of Technology, Guangzhou 510006, China

*Corresponding author: **Prof. Xun-an Ning.**

Tel.: +86-20-3932 2546; Fax: 86-20-3932 2548; Email: ningxunan666@126.com; 1009560924@qq.com.

List of Contents:

Text S1 Experimental procedure.

Text S2 Analytical methods.

Table S1 Relative content of elements in the solid phase of simulated sludge (expressed in oxide form).

Table S2 Name, structure, retention time, and characteristic ions of Phe products after Fenton/Cl^- treatment identified by the GC-MS. Fenton/Cl^- conditions: pH=3.0; H_2O_2/Fe^{2+}=1:1; H_2O_2=120 mM; reaction time=1-30 min; 4000 mg/L Cl^-.

Table S3 Ecotoxicity of Phe and its products

Table S4 Intermediate products of Phe degradation in different reaction systems

Fig. S1 Effects of Cl^- concentration and pH on the removal of free-radical probes (NB, BA, and TBA) from the simulated sludge liquid phase using an Fenton/Cl^- system. The first-order rate constants of free-radical probe removal are also provided (a,c,e: pH=3.0, Fe^{2+}/H_2O_2=1/1, H_2O_2=30 mM; b,d,f: Cl^- =1000 mg/L, Fe^{2+}/H_2O_2=1/1, H_2O_2=30 mM).

Fig. S2 Extracted-ion mass chromatographs for the products of Phe obtained from the Fenton/Cl^- treatments.

Fig. S3 Mass spectra of the fragments of Phe degradation products obtained during the Fenton/Cl^- treatment.

Fig. S4 Distribution of main Phe products in the Fenton/Cl^- process.

Text S1 Experimental procedure.

Considering the investigation of PAH content in actual TDS from Guangdong (Ning et al., 2014), and the water solubility of PAHs, 5 ml of dichloromethane and 10 μg each of Phe, Ant and Flu were added to 1 g of simulated sludge solid phase. The mixture was aged for 24 h to obtain the solid phase of simulated sludge containing PAH. Then, ultrapure water was employed to introduce a water content of 98% to the simulated PAH-containing sludge. The pH (3.0-5.0) of the system was adjusted using H_2SO_4, a typical acid conditioner for sludge conditioning tank (epoxy cement tank or enamel reactor), and anhydrous sodium acetate (Jonsson et al., 2007; Wang et al., 2019). The Phe, Ant, and Flu contents in the solid phase of the system with 98% water content were 1767.60±239.18, 3370.18±272.36, and 4575.17±474.64 ng/g, respectively.

In the early stages, we used Fenton to degrade the PAHs within the simulated sludge and determined the optimal operating conditions of the Fenton system (Lai et al., 2020). Based on these optimal conditions ($H_2O_2/Fe^{2+}=1/1$, $H_2O_2=30$ mM), the effects of pH (3.0, 4.0, and 5.0), Cl^- concentration (50, 100, 500, 1000, and 2000 mg/L), and reaction time (5, 10, 20, 30, and 40 min) on the removal of PAHs from simulated sludge solid phase using the Fenton/Cl^- system were further investigated. In addition, when the TBA concentration was 135 mM, or that of BQ was 10 mM, PAHs in simulated sludge solid phase were degraded by the Fenton/Cl^- system ($H_2O_2/Fe^{2+}=1/1$, $H_2O_2=30$ mM, 40 min, $Cl^-=50$-2000 mg/L, pH=3.0-5.0). DMPO in DMSO was also degraded by the Fenton/Cl^- system ($H_2O_2/Fe^{2+}=1/1$, $H_2O_2=30$ mM, 3 min, $Cl^-=50$-2000 mg/L, pH=3.0-5.0).

NB (19.14 μg/mL), BA (40.00 μg/mL), and TBA (31.00 μg/mL) were added to the liquid phase of the simulated sludge system with 98% water content. The adsorption kinetics of free-radical probes (NB, BA, and TBA) by simulated sludge solid phase at different pH values (3.0, 4.0, and 5.0) were investigated. In addition, the free-radical probes in the liquid phase were degraded by the Fenton/Cl^- system ($H_2O_2/Fe^{2+}=1/1$, $H_2O_2=30$ mM, 0.5-30 min, Cl^- =50-2000 mg/L, pH=3.0-5.0) and their removal kinetics were explored.

Simulated sludge solid phase (1 g) was added to 5 mL of dichloromethane, followed by 1 mg of Phe. Using the same preparation method, simulated sludge containing a water content of 98% and a high concentration of Phe was prepared. Then, Phe was degraded by the Fenton/Cl^- system ($H_2O_2/Fe^{2+}=1/1$, $H_2O_2=120$ mM, 5-30 min, Cl^- =4000 mg/L, pH=3.0).

The reaction was carried out at normal temperature. The mixing speed of the reaction system was controlled at 300 rpm using a magnetic mixer. The Fenton/Cl^- system was quenched with excess sodium hyposulfite (105% of the required stoichiometric ratio). After the reaction, the samples were centrifuged (4000 rpm, 5 min) and the solid samples were freeze-dried at -60 □ for 24 h while the liquid samples were filtered and stored at 4 □.

Text S2 Analytical methods.

The chemical composition of the simulated sludge solid phase was determined using an energy dispersive X-ray fluorescence (XRF) spectrometer (EDX-7000, China). The pH values of the samples were determined using a digital pH meter (pHS-3C, China). The concentration of free chlorine was calculated at 515 nm (HJ 586-2010) using an ultraviolet spectrophotometer (Cary 100, Agilent, USA). Electron paramagnetic resonance (EPR) analysis was performed using an EMXplus-10/12 spectrometer (Bruker, Germany). The working parameters of EPR were as follows: scanning width, 100 G; center field, 3512 G; microwave frequency, 9.85 GHz; microwave power, 20 mW; and temperature, 25 ℃. Methanol and ultrapure water were used as the mobile phase (1 mL/min) for high-performance liquid chromatography (HPLC, SHIMADZU LC-16). The concentrations of NB and BA in the sample liquid phase were determined by HPLC at 266 nm and 235 nm, respectively, and the chromatographic separation was achieved using a C-18 column (Poroshell, 4.6×50 mm, 2.7 μm). The concentration of TBA in the sample liquid phase was determined using a purge and trap concentrator and gas chromatography-mass spectrometry (GC-MS, ATOMX-7890B-5977B, Agilent, USA). The operating parameters for GC-MS quantitative analysis of TBA were as follows: inlet temperature, 250 ℃; carrier gas, highly pure helium (16.2 mL/min); and shunt flow rate, 12 mL/min. The initial temperature was 40 ℃ (held for 1 min), which was increased at a rate of 10 ℃/min to 240 ℃ where it was held for 1 min.

Phe and its products in the sample liquid phase were extracted with a 1/4 (v/v) dichloromethane/*n*-hexane mixed solution (Lai et al., 2019). The PAHs and Phe products in the sample solid phase were extracted by ultrasound (JY92-IIN, Ningbo Science Biotechnology, China) with a 1/1 (v/v) dichloromethane/acetone mixed solution (Lin et al., 2016). The extracted solutions were treated with anhydrous sodium sulfate to remove water and particulate matter. Then, the extracted solutions were concentrated to 1 mL.

GC-MS was used to quantitatively analyze the PAHs and qualitatively analyze the Phe nonpolar products. In addition, 1 mL of the concentrated sample was dried with nitrogen, 50 μL of BSTFA and 50 μL of pyridine were added to the sample, and the sample was derivatized at 60 □ for 30 min. The sample was then re-dissolved with *n*-hexane and dichloromethane, and finally the polar Phe products were analyzed by GC-MS.

The operating parameters for quantitative analysis of PAHs by GC-MS: the inlet temperature was 280 □, and the carrier gas (34 mL/min) was highly pure helium. Temperature conditions: the initial temperature was 80 □ (held for 1 min), rising to 161 □ at a rate of 3 □/min, then rising to 220 □ at a rate of 5 □/min, and finally rising to 280 □ at a rate of 20 □/min (held for 2 min).

The operating conditions of GC-MS qualitative analysis: the inlet temperature was 280 □, and the carrier gas (50 mL/min) was highly pure helium. Temperature conditions: the initial temperature was 35 □ (held for 3 min), rising to 220 □ at a rate of 10 □/min (held for 3 min), and finally rising to 280□ at a rate of 20 □/min (held for 5 min).

Table S1 Relative content of elements in the solid phase of simulated sludge (expressed in oxide form).

	Ignition loss (%)	Relative content of elements (%)					
		Fe_2O_3	SO_3	SiO_2	P_2O_5	CaO	Other
Simulated sludge	16.54 ± 0.37	56.38 ± 0.37	12.46 ± 0.07	6.43 ± 0.09	3.70 ± 0.05	2.82 ± 0.03	1.67 ± 0.05

Table S2 Name, structure, retention time, and characteristic ions of Phe products after Fenton/Cl$^-$ treatment identified by the GC-MS. Fenton/Cl$^-$ conditions: pH=3.0; H_2O_2/Fe^{2+}=1:1; H_2O_2=120 mM; reaction time=1-30 min; 4000 mg/L Cl$^-$.

Non-derivatization product/Derivative product	Liquid/Solid phase	Objective/ Products (chemical formula)	Structure	Retention time (min)	Characteristic ions (m/z)
Non-derivatization product	Solid phase	Phenanthrene ($C_{14}H_{10}$)	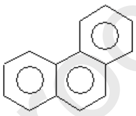	19.542	178,176,179,76
Non-derivatization product	Liquid phase and solid phase	2,5-Dimethyltetrahydrofuran ($C_6H_{12}O$)	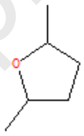	3.230	56,41,85,43
Non-derivatization product	Liquid phase	2-Furanmethanol ($C_5H_{10}O_2$)	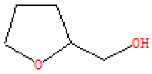	4.372	71,43,41,27
Non-derivatization product	Liquid phase	2,4-di-*tert*-butylphenol ($C_{14}H_{22}O$)	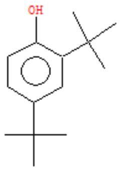	16.349	191,57,206,192
Derivative product	Liquid phase and solid phase	3,7-dioxa-2,8-disilanonane ($C_7H_{25}O_3$)	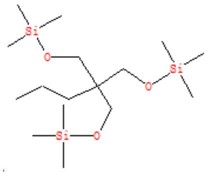	17.844	191,31,73,44
Non-derivatization product	Liquid phase	Diphenaldehyde ($C_{14}H_{10}O_2$)	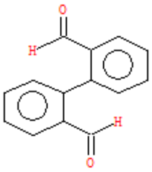	20.448	181,152,153,182
Non-derivatization product	Solid phase	9-Phenanthrenol ($C_{14}H_{10}O$)	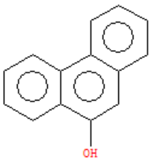	23.617	165,194,166,82

Table S3 Ecotoxicity of Phe and its products

Objective/ Products (chemical formula)	Octanol-water partition coefficient (atm m^3/mol)	Acute toxicity (mg/L)			Chronic toxicity (mg/L)		
		Fish (LC$_{50}$)	Daphnid (LC$_{50}$)	Green Algar (EC$_{50}$)	Fish	Daphnid	Green Algar
Phenanthrene ($C_{14}H_{10}$)	4.50	0.83	0.60	1.15	0.11	0.11	0.50
2,5-Dimethyltetrahydrofuran ($C_6H_{12}O$)	1.77	131.85	73.30	50.05	12.57	6.74	12.51
2-Furanmethanol ($C_5H_{10}O_2$)	0.45	697.06	489.26	117.57	44.23	55.01	39.28
2,4-di-*tert*-butylphenol ($C_{14}H_{22}O$)	4.80	0.27	0.28	0.98	0.04	0.05	0.04
3,7-dioxa-2,8-disilanonane ($C_7H_{25}O_3$)	0.68	1866.17	938.04	422.15	157.99	65.16	84.27
Diphenaldehyde ($C_{14}H_{10}O_2$)	3.19	1.52	1.42	0.34	0.04	0.11	0.16
9-Phenanthrenol ($C_{14}H_{10}O$)	3.87	1.29	0.89	3.42	0.17	0.17	1.57

Table S4 Intermediate products of Phe degradation in different reaction systems

Compound	Structure	Oxidation process (dominant reactive species)			
		Fenton (·OH)^a	UV/TiO_2 (·OH)^b	Iron-based catalytic materials/sodium persulfate (sulfate radical)^c	Fenton/Cl^-: this study
9-Phenanthrol	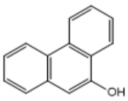		√	√	√
9,10-Phenanthrenequinone	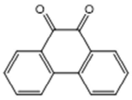		√	√	
2,3-Phenanthrenequinone	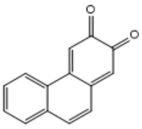			√	
2,2’-Biphenyldicarboxylic anhydride	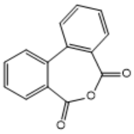			√	
3,4-Benzocoumarin	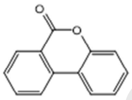		√		
Diphenaldehyde	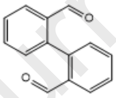		√	√	√
2,2-Biphenyldicarbaldehyde	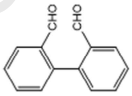			√	
Naphthaldehyde	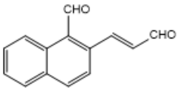			√	
Phtalic acid	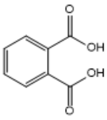	√			
Phtalic anhydride	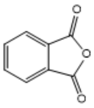	√			
Acetylbenzoyl	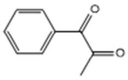	√			

2,4-di-*tert*-butylphenol	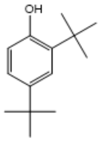			√

[a] 15 g/L H_2O_2, H_2O_2/Fe^{2+}=10:1, 6-8 mg/L Phe, 20-60 □, pH=2.5, liquid phase (water and methanol) (Bendouz et al., 2017); [b] 100 mg/L TiO_2, UV=365 nm, UVA=3.9 Mw/cm^3, UVB=1.1 Mw/cm^3, UVC=0.3 Mw/cm^3, 10 mg/L Phe, 25 □, pH=6.0-8.0, liquid phase (water and acetone) (Woo et al., 2009); [c] 50 mg/L iron-based catalytic materials, 0.3 mM sodium persulfate, 1 mg/L Phe, 20 □, pH=2.0-10.0, aqueous phase (Gu et al., 2018).

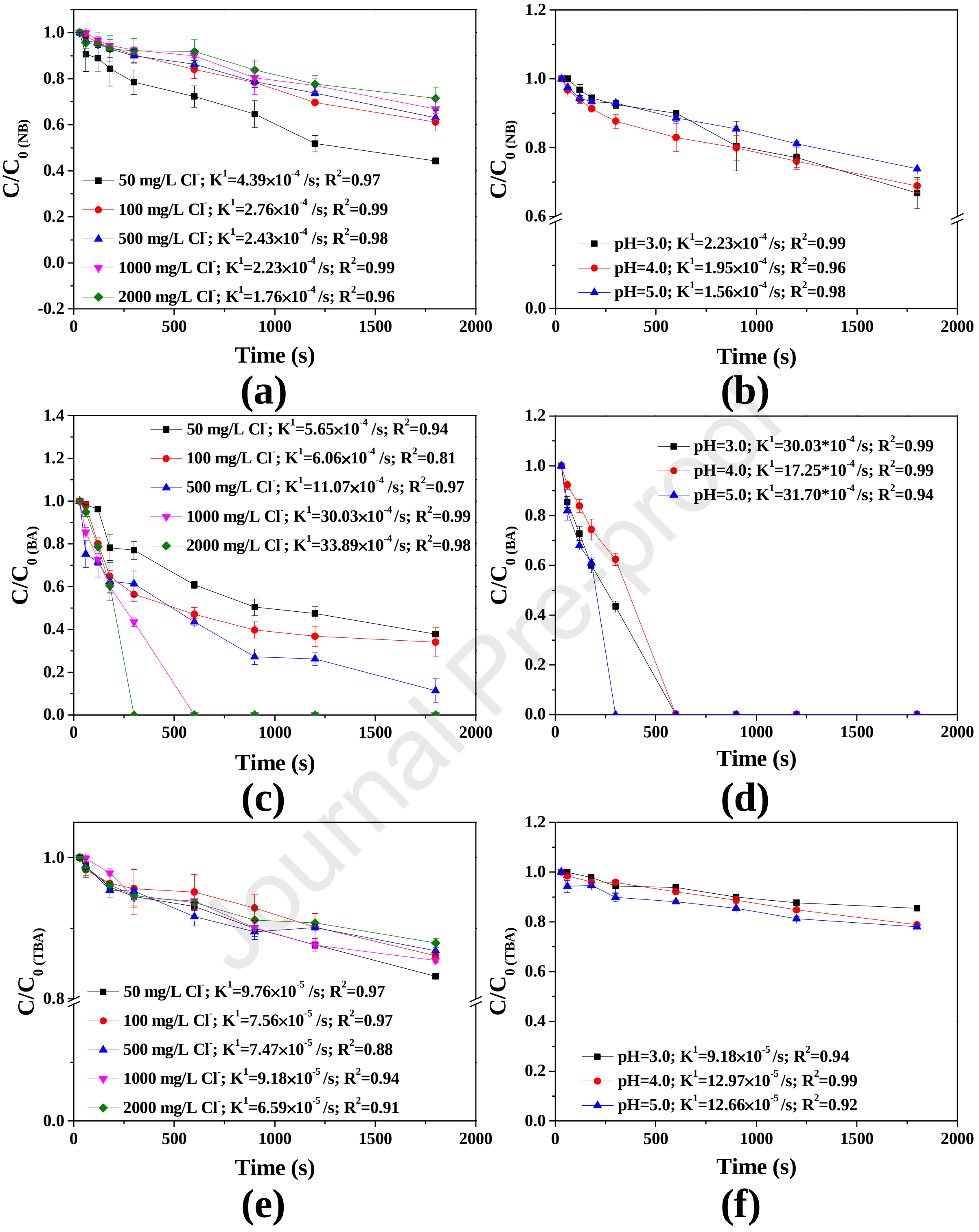

Fig. S1 Effects of Cl^- concentration and pH on the removal of free-radical probes (NB, BA, and TBA) from the simulated sludge liquid phase using an Fenton/Cl^- system. The first-order rate constants of free-radical probe removal are also provided (a,c,e: pH=3.0, Fe^{2+}/H_2O_2=1/1, H_2O_2=30 mM; b,d,f: Cl^-=1000 mg/L, Fe^{2+}/H_2O_2=1/1, H_2O_2=30 mM).

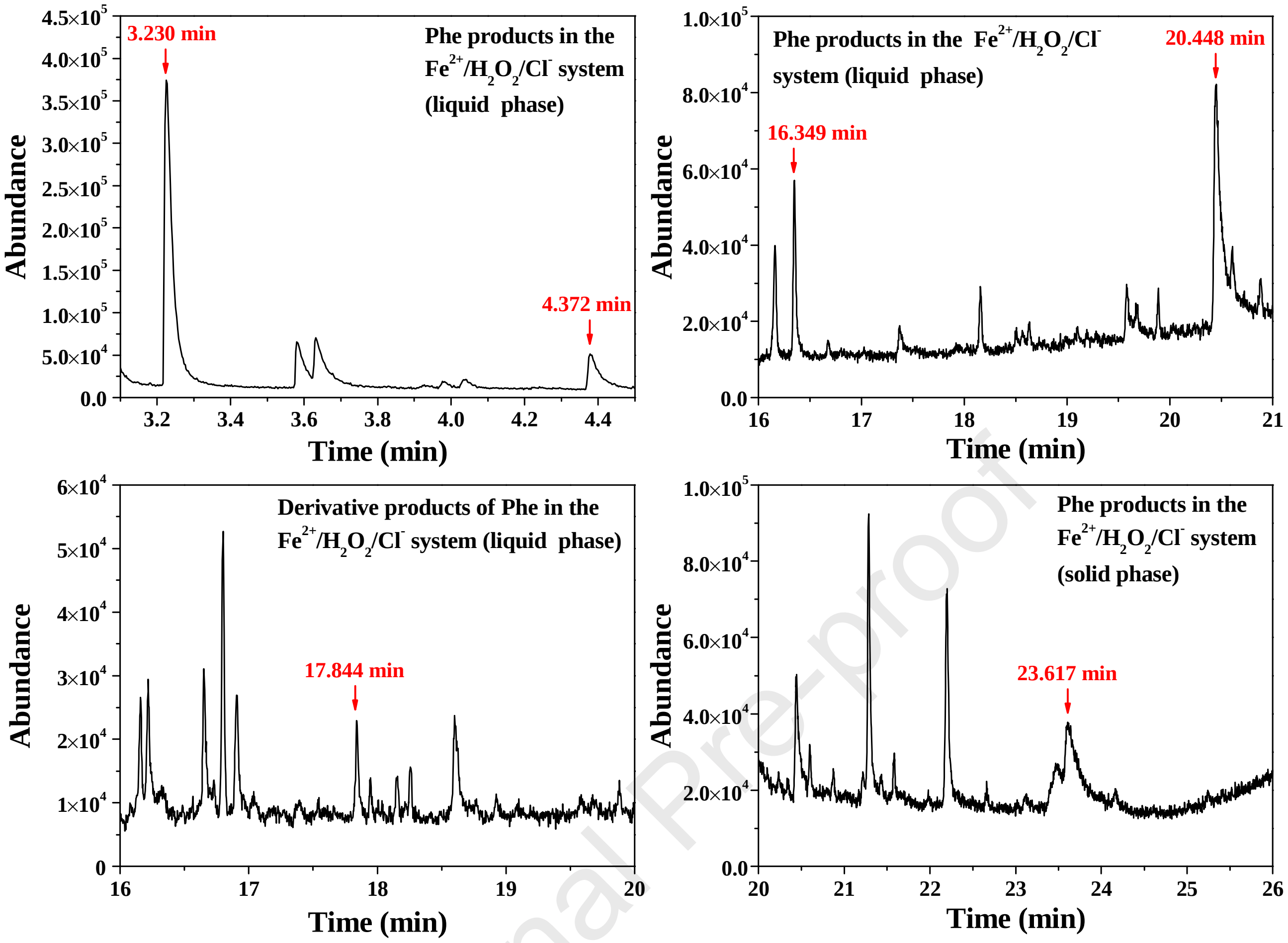

Fig. S2 Extracted-ion mass chromatographs for the products of Phe obtained from the Fenton/Cl$^-$ treatments.

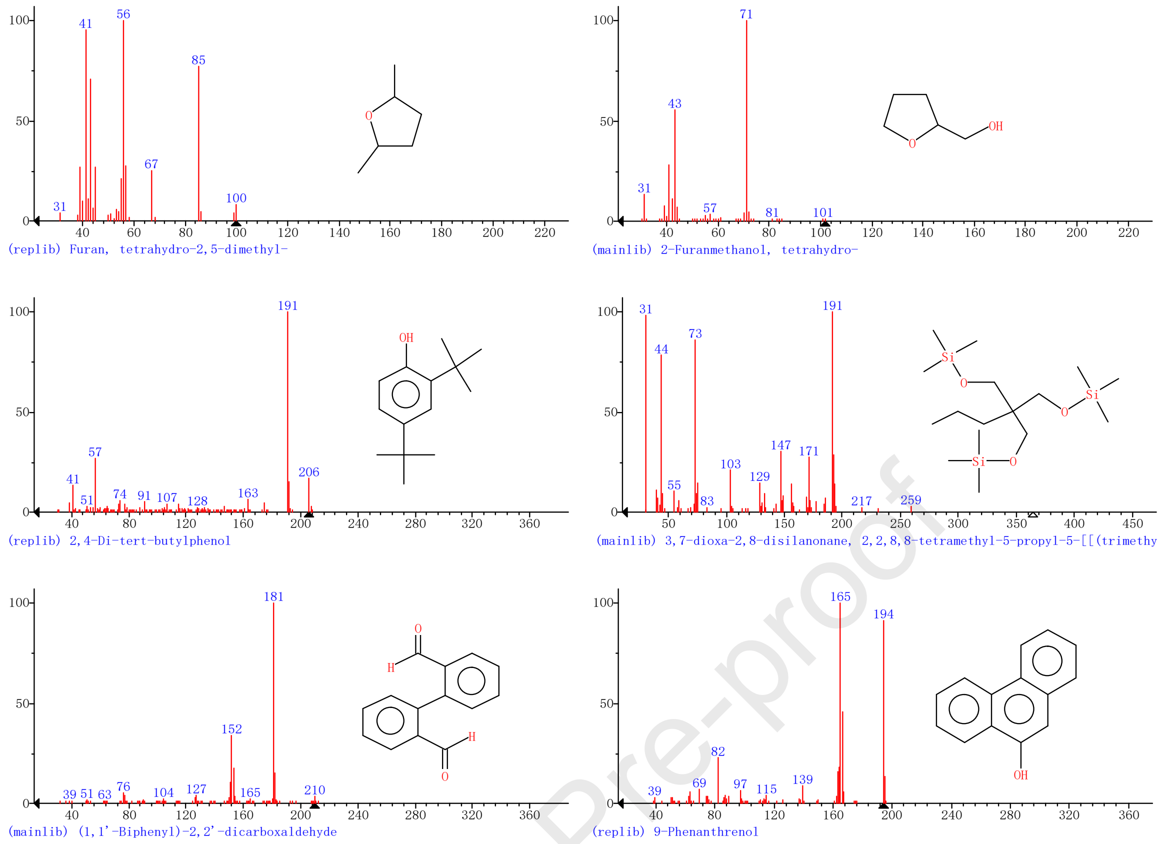

Fig. S3 Mass spectra of the fragments of Phe degradation products obtained during the Fenton/Cl$^-$ treatment.

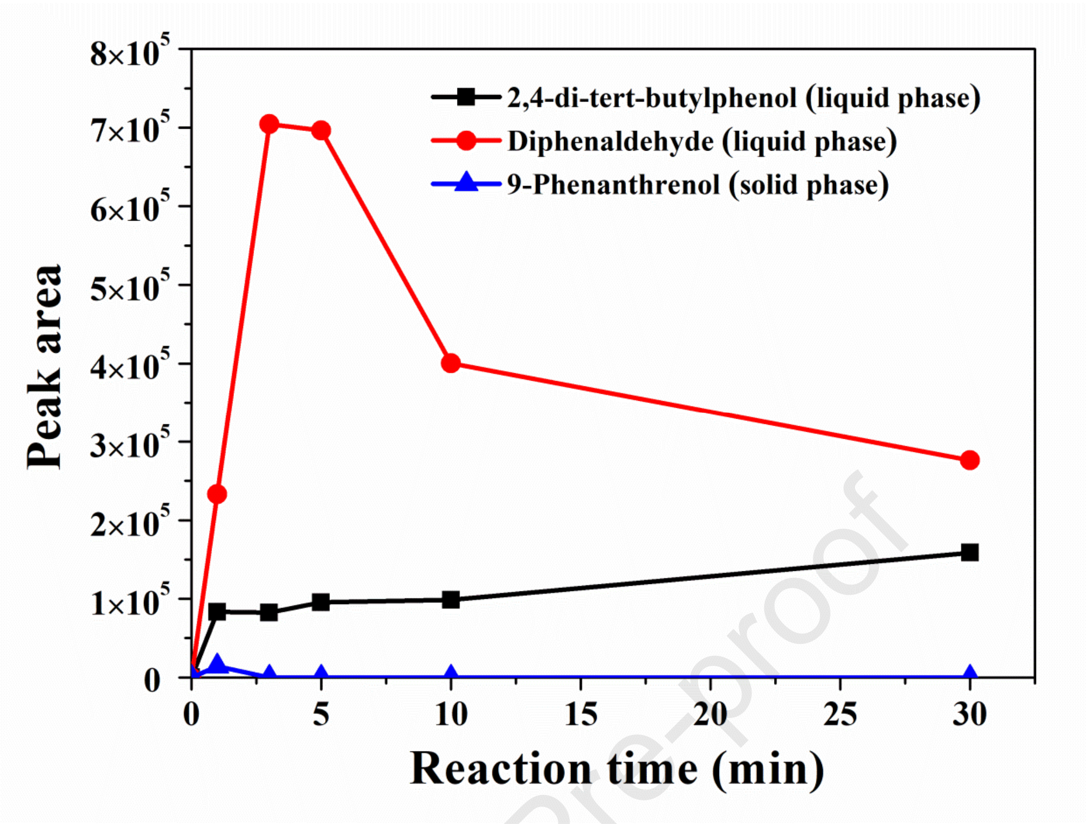

Fig. S4 Distribution of main Phe products in the Fenton/Cl^- process.

References

Bendouz, M., Tran, L.H., Coudert, L., Mercier, G., Blais, J.F., 2017. Degradation of polycyclic aromatic hydrocarbons in different synthetic solutions by Fenton's oxidation. Environ. Technol. 38, 116-127.

Gu, M.B., Sui, Q., Farooq, U., Zhang, X., Qiu, Z.F., Lyu, S.G., 2018. Degradation of phenanthrene in sulfate radical based oxidative environment by nZVI-PDA functionalized rGO catalyst. Chem. Eng. J. 354, 541-552.

Jonsson, S., Persson, Y., Frankki, S., van Bavel, B., Lundstedt, S., Haglund, P., Tysklind, M., 2007. Degradation of polycyclic aromatic hydrocarbons (PAHs) in contaminated soils by Fenton's reagent: A multivariate evaluation of the importance of soil characteristics and PAH properties. J. Hazard. Mater. 149, 86-96.

Lai, X.J., Ning, X.A., Chen, J.Y., Li, Y., Zhang, Y.P., Yuan, Y.Q., 2020. Comparison of the Fe^{2+}/H_2O_2 and Fe^{2+}/PMS systems in simulated sludge: Removal of PAHs, migration of elements and formation of chlorination byproducts. J. Hazard. Mater. 398, 122826.

Lai, X.J., Ning, X.A., He, Y., Yuan, Y.Q., Sun, J., Ke, Y.W., Man, X.Y., 2019. Treatment of a simulated sludge by ultrasonic zero-valent iron/EDTA/Air process: Interferences of inorganic salts in polyaromatic hydrocarbon removal. Waste Manage. 85, 548-556.

Lin, M.Q., Ning, X.A., An, T.C., Zhang, J.H., Chen, C.M., Ke, Y.W., Wang, Y.J., Zhang, Y.P., Sun, J., Liu, J.Y., 2016. Degradation of polycyclic aromatic hydrocarbons (PAHs) in textile dyeing sludge with ultrasound and Fenton processes: Effect of system parameters and synergistic effect study. J. Hazard. Mater. 307, 7-16.

Ning, X.A., Lin, M.Q., Shen, L.Z., Zhang, J.H., Wang, J.Y., Wang, Y.J., Yang, Z.Y., Liu, J.Y., 2014. Levels, composition profiles and risk assessment of polycyclic aromatic hydrocarbons (PAHs) in sludge from ten textile dyeing plants. Environ. Res. 132, 112-118.

Wang, Z., Qiu, W., Pang, S.Y., Jiang, J., 2019. Effect of chelators on the production and nature of the reactive intermediates formed in Fe(II) activated peroxydisulfate and hydrogen peroxide processes. Water Res. 164, 114957.

Woo, O.T., Chung, W.K., Wong, K.H., Chow, A.T., Wong, P.K., 2009. Photocatalytic oxidation of polycyclic aromatic hydrocarbons: Intermediates identification and toxicity testing. J. Hazard. Mater. 168, 1192-1199.

Declaration of interests

☑ The authors declare that they have no known competing financial interests or personal relationships that could have appeared to influence the work reported in this paper.

☐ The authors declare the following financial interests/personal relationships which may be considered as potential competing interests: